




H. Montazer Hojjat · S. Kozinov · D. Balzani 

An a priori irreversible phase-field formulation for ductile fracture at finite strains based on the Allen–Cahn theory: a variational approach and FE-implementation

Received: 19 April 2023 / Accepted: 20 November 2023 / Published online: 12 January 2024
© The Author(s), under exclusive licence to Springer-Verlag GmbH Germany, part of Springer Nature 2024

Abstract In this paper, a new crack surface energy for the simulation of ductile fracture is proposed, which is based on the Allen–Cahn theory of diffuse interfaces. In contrast to existing fracture approaches, here, the crack surface energy density is a double-well potential based on a new interpretation of the crack surface. That is, the energy associated with the whole diffuse region between the fully cracked and intact regions is interpreted as crack surface energy. This kind of formulation, on the one hand, results in the balance of micromechanical forces and on the other hand, is a priori thermodynamically consistent. Furthermore, the proposed formulation is based on a gamma-convergent interface energy and it is in agreement with the classical solution of Irwin (Appl Mech Trans ASME E24:351–369, 1957). It is shown that in contrast to existing models, crack irreversibility is automatically fulfilled and no further constraints related to neither local nor global irreversibility are needed. To also account for potential plastic shear band localization, the approach is extended by a micromorphic plasticity model. By analyzing two different classical numerical benchmark problems, the proposed formulation is shown to enable mesh-independent results which are in agreement with the results of competing approaches.

Keywords Ductile phase-field fracture · Micromorphic extension · Finite strains · Crack irreversibility · Balance of micro-forces · Γ -convergence

1 Introduction

Prediction of crack initiation and the way it propagates in the engineering structures has been a big challenge during the past decades. As an example, in the mechanized tunneling, the cutting disks are subject to fracture. Since these tools are mainly constructed from ductile steels, they are subject to ductile fracture. The study of crack goes back to the end of the 19th century when Kirsch [33] studied the stress concentration around a circular hole subject to crack initiation. Similarly, Inglis [28] studied the stress field around a flat elliptical hole, regarding it as a crack. His approach resulted in infinite stresses at the crack tip, in the limit of a perfectly sharp crack. This mathematical flaw, was eliminated in the energy-balance approach proposed by [21]. Based on this classical approach, two energy-free triangular-like regions at the top and bottom of the crack are considered to be formed. Considering these energy-free regions, an increase in the crack length results in a more released energy. Furthermore, new crack surfaces are created, and the crack surface energy increases. Using this approach and taking the first variation of the total energy with respect to the crack length, one can find a critical crack length, for which the crack propagates spontaneously. This is the case observed in the fracture of brittle materials. Griffith defined the material constant $g_c = 2\gamma$, which is indeed the critical energy dominating the cohesive forces, where γ is crack surface energy per unit length. Later, Orowan [56] stated, that this parameter is inadequate to describe fracture in ductile materials. He proposed that the plastic work

(w_p) plays a dominant role. Taking this into account, [29] modified the Griffith approach. He stated that the release of strain energy is not only dissipated by the propagated crack's surface energy, but also by the plastic work in the vicinity of the crack tip. In his modification, he introduced the modified Griffith parameter, taking the plastic work into account

$$g_c^{\text{Irwin}} = 2\gamma + w_p. \quad (1)$$

Although these studies established the foundation of fracture mechanics, they are unable to predict the crack path and to elucidate crack kinking or branching. This flaw is addressed and removed in the so-called classical Finite Fracture Mechanics (FFM). One of the first authors who introduced the concept of FFM was Hashin [26], where the formation of many cracks of finite surface in a very short time is considered. Leguillon [41] used this framework and defined a double-condition criterion to be fulfilled simultaneously for the onset of brittle fracture. The two necessary conditions (also called coupled criterion) are an energy condition analogous to Griffith approach and a stress condition for the formation of a crack of finite size, i.e., the stress that a material can undergo before it breaks. The first condition results in a lower bound of admissible crack length whereas the second criterion defines an upper bound according to [41]. Within this framework, the stress and energy flux are analyzed at a finite distance from the crack tip. This distance is assumed to be small enough compared to the geometrical size of the specimen and prescribed as a structural parameter rather than a material constant according to [13]. However, this approach is very sensitive to the estimated material properties where the critical tension can be highly affected by the preexisting micro-cracks or voids within the specimen [67]. The interested reader is referred to the review by [70].

Different numerical techniques have been developed to overcome the aforementioned flaw. A classical approach to simulate fracture is based on its description in terms of strong discontinuities, cf. e.g., Simo et al. [64]. In this context, the finite elements are divided where the crack propagates. However, aside from a quite sophisticated implementation, this method lacks generality and causes complications for, e.g., crack branching. The other common method is the Extended Finite Element Method (XFEM), developed by [8]. This method is based on adding local enrichment functions into finite element formulations using the partition of unity concept. In this framework, a crack is defined implicitly using level sets that result in crack propagation independent from the underlying finite element mesh. Although this method is mesh-independent, it has its own disadvantages. Topology definition using level set functions increases numerical complexity, specifically for 3D cracks, crack kinking or branching. In addition to that, using the enrichment coefficients as additional degrees of freedom increases the computational cost.

Another class of approaches considers the crack not as a strong discontinuity, but rather in a smeared sense. This can be directly described in terms of continuum damage mechanics formulations. However, a major problem thereof is that the strongly damaged zones, which are interpreted as the crack, localize and the structural simulation becomes mesh-dependent. Therefore, gradient-enhanced formulations were developed, for instance based on ideas in [15] to enable mesh-independent calculations. There, the damage field is considered as a separate variable whose gradient is additionally included in the energy density function. c.f. [58], [69] The additional field leads to an increased number of degrees of freedom in associated finite element calculations. However, significant improvements with regard to efficiency could be obtained in [30] for the geometrically linear case and in [31] for the nonlinear setting, see also [61] which allows for a simple implementation in terms of standard finite element interfaces. An alternative to gradient damage formulations based on convexification of incremental stress potentials at the integration points is proposed in [7]. This so-called relaxation approach does not require additional primary variables in finite element implementations and it still allows for mesh-independent calculations of damage. This approach has been extended to describe sophisticated stress-softening hysteresis of soft biological tissues in [62] and to strain softening in [34]. Another approach, where the crack is not considered as strong discontinuity, is based on eroding those finite elements which represent the crack. The eigerosion method, which was initially proposed by Pandolfi and Ortiz [57] stemmed from the work of Francfort and Marigo [20] and provided a suitable framework for the mesh-independent modeling of crack propagation. There, the net gained energy defined as the difference between the potential energy and the effective crack surface energy is computed and based thereon, any element with the highest positive net gained energy is eroded in an iterative process. Wingender and Balzani [72] extended this method to simulate crack propagation in ductile materials undergoing large deformations, see also [71] for an extension to crack propagation through heterogeneous structures. However, the nonlocal normalization of the crack surface as major part of the eigerosion concept, requires information from neighboring finite elements and thus, a rather sophisticated implementation.

Phase-field fracture is another example of continuous methods, which has gained a lot of attention in the mechanics' society in the past decade and which shares strong analogies with micromorphic gradient damage approaches, see e.g., [38,39]. This method, which goes back to the work of Francfort and Marigo [20], is based on two pillars. Those are the Griffith balance of energy and the continuum description of the crack. In this framework, the displacement field is considered continuous across the crack using a phase-field parameter. A direct link to the continuum mechanics, on the one hand, and a straightforward implementation in finite element (FE) packages, render this method as a robust one. However, discretized forms of existing formulations, cf. Karma et al. [32], Hakim and Karma [25], Bourdin [10], Miehe et al. [47], Miehe et al. [50], are not proven to be both Γ -convergent and thermodynamically consistent. Γ -convergence is, however, important in order to ensure that the smeared crack yields the discrete crack in the limit and that stable minimizers are obtained in the presence of continuous perturbations. In this paper, based on a modified crack definition, a modification to the phase-field fracture approach is presented. The resulting formulation is consistent with both the Allen–Cahn theory of diffusive interfaces and the Irwin's classical model. Furthermore, a new crack surface energy density functional is used, whose counterpart in the context of phase transformation has been proven to be Γ -convergent [11,52]. Furthermore, the proposed formulation for ductile fracture at finite strains is thermodynamically consistent. The method is implemented using a user element (UEL) in ABAQUS. Two numerical benchmark experiments are carried out. The paper is organized as follows: Sect. 2 deals with the phase-field theory, its origination and a short overview of micro-forces. In Sect. 3, a short summary of existing approaches with respect to Γ -convergence and with regard to the incorporation of fracture irreversibility is provided, which is followed by the proposed phase-field approach, where fracture irreversibility is a priori fulfilled. In addition to that, this section proposes a further micromorphic extension for ductile fracture and provides a description of a monolithic algorithmic implementation. Finally, to illustrate the performance of the proposed formulation, in Sect. 4 two numerical benchmark problems are investigated and the results are discussed. In Sect. 5 the proposed formulation is summarized and argued.

2 Recapitulation of phase-field approaches

In order to put the extensions proposed in this paper in perspective to existing phase field approaches, it is important to recapitulate the fundamental ideas of the major phase-field fracture models in connection with similar approaches in a diffusion context. Starting point of phase field fracture models is a fundamental idea in the context of phase transformation phenomena. There, a phase-field parameter is defined to represent sharp interfaces in a smeared manner. The model proposed in this paper is constructed in line with the original Allen–Cahn theory, which is why we recapitulate briefly the main idea. The classical approach is based on diffusion theory to model material properties of a media consisting of more phases, cf. e.g., [66]. The phase-field theory was mainly developed by [12] and [4], where the latter is considered here. The Allen–Cahn theory of diffusive interfaces was proposed to compute the interface energy in an inhomogeneous region between two phases, α and β . In this theory, a phase-field parameter p , or the so-called order parameter, is introduced. This parameter is equal to c for phase α and $-c$ for phase β . These two values are the minimizer of a free energy density f_0 of a homogeneous phase which is thus, considered to be a double-well functional. In other words, the lowest energy states are given by the first variation of this energy functional with respect to the order parameter, i.e., $\delta_p f_0 = \frac{\partial f_0}{\partial p} \delta p = 0$. The physical space between these two energetic minimum states is defined as the interface, and its length is equal to the atomistic interface length $l_s = 2c$ [66]. Within this space, the order parameter possesses values between $-c$ and c ($-c \leq p \leq c$). Any change of order parameter from the infimum states would increase f_0 . Therefore, an increment Δf_0 can be defined as the difference of free energy between a homogeneous state of arbitrary order parameter and those infimum states $p = -c$ and $p = c$ [4]. Based thereon, an excess energy density is defined as

$$\Delta f(p, \nabla p) = \Delta f_0(p) + 2\theta(\nabla p)^2. \quad (2)$$

This energy appears as homogenization of microstructure, where a mixture of the two states exists. Therefore, it is assumed that aside from the local point also the neighboring microstructure contributes to the response, which is why the gradient of the order parameter is also included. The parameter θ is the associated material constant. By integrating over the physical domain of the body, the total excess energy reads

$$\Delta F(p, \nabla p) = \int_{\Omega} \Delta f(p, \nabla p) dV. \quad (3)$$

Based on the excess energy density defined in equation (2) and considering the micromechanical stress Υ and the internal micromechanical force π , the reduced dissipation inequality results in [24]

$$\mathcal{D} = -\Delta \dot{f} - \pi \dot{p} + \Upsilon \cdot \nabla \dot{p} \geq 0, \quad (4)$$

where the micromechanical stress and internal force are conjugated to the order parameter and its gradient, respectively. The micromechanical dissipation inequality can be rewritten as

$$\left(\frac{\partial \Delta f}{\partial p} + \pi \right) \dot{p} + \left(\frac{\partial \Delta f}{\partial \nabla p} - \Upsilon \right) \cdot \nabla \dot{p} \leq 0. \quad (5)$$

In order to fulfill this inequality for any arbitrary process, the micromechanical stress vector reads

$$\Upsilon = \partial_{\nabla p} \Delta f(p, \nabla p). \quad (6)$$

Therefore, inequality (5) simplifies to

$$\underbrace{\left(\frac{\partial \Delta f}{\partial p} + \pi \right)}_{\pi_{\text{dis}}} \dot{p} \leq 0. \quad (7)$$

For the statical case, where $\dot{p} = 0$, $\pi_{\text{dis}} = 0$ is considered which yields

$$\pi = -\frac{\partial \Delta f}{\partial p}. \quad (8)$$

Taking the variation of the excess free energy with respect to the order parameter to be zero, applying divergence theorem and partial integration, the Euler–Lagrange equations at the micromechanical level are obtained as

$$\nabla \cdot \Upsilon + \pi = \xi \quad (9)$$

Herein, ξ denotes external micromechanical forces which may be considered zero. For the dynamic case where p is allowed to evolve, the inequality (7) can be a priori fulfilled if π_{dis} is assumed to have the general form [24]

$$\pi_{\text{dis}} = -\frac{\kappa}{2} \dot{p}, \quad (10)$$

where κ is a non-negative modulus interpreted as kinetic modulus. Then, the micromechanical dissipation reads

$$\mathcal{D} = \frac{1}{2} \kappa \dot{p}^2 \geq 0. \quad (11)$$

Then, the Allen–Cahn equation of interface motion is obtained by minimizing the sum of excess energy and dissipation. According to the static case, we set the variation with respect to p equal to zero, apply the divergence theorem and partial integration, and obtain the Euler–Lagrange equation

$$\nabla \cdot \Upsilon - \frac{\partial \Delta f}{\partial p} = \xi + \frac{\partial \mathcal{D}}{\partial \dot{p}}. \quad (12)$$

Again, the micromechanical forces ξ are usually considered to be zero. Then, this Euler–Lagrange equation is equivalent to

$$\frac{\partial p}{\partial t} = -\beta \frac{\partial \Delta f_0}{\partial p} + 4\beta\theta \nabla \cdot \nabla p, \quad (13)$$

where $\beta = \frac{1}{\kappa}$ is a positive kinetic constant interpreted as viscosity or mobility of the interface [53]. This equation is also referred to as the time-dependent Ginzburg–Landau equation in the literature [24].

Due to the presence of sharp interfaces in case of cracks, it appears reasonable to apply the major idea of smearing out the sharp crack using an order parameter. Therefore, a variety of different approaches have been proposed in the past two decades. Taking crack surface and bulk energies into account in a variational setting, [20] studied crack propagation for a quasi-static problem in a brittle material. Later on, [10] suggested a regularized approximation of the proposed variational formulation. This was performed by introducing an auxiliary crack parameter, which interpolates between the cracked and fully intact regions. Subsequently, [47] proposed a thermodynamically consistent phase-field fracture model introducing an irreversibility condition. This method has been further developed by different authors to simulate crack propagation for small and finite strains in a wide range of materials, including metals, concretes, soft tissues, etc., cf. Gültekin et al. [22,23], Msekhi et al. [54], Miehe and Schänzel [46], Miehe et al. [50], Spetz et al. [65], Aldakheel et al. [2], Aldakheel et al. [3], Raina and Miehe [60], Ambati et al. [5], Ambati et al. [6].

As already mentioned in the Introduction, the phase-field fracture method is based on two pillars, the Griffith balance of energy and the continuum description of the crack. The Griffith balance of energy states that the crack surface energy increases to the same amount as the bulk energy reduces as soon as the crack propagates. In a first step, an auxiliary parameter (d) is defined. This parameter is interpreted as a damage parameter smoothening the transition between two phases α and β . The phase α represents the intact zone and the phase β the fully cracked region. Therefore, values zero and one are assigned to the parameter d at each phase, respectively

$$d = \begin{cases} 0 & \text{intact region, phase } \alpha, \\ 1 & \text{fully cracked, phase } \beta. \end{cases} \quad (14)$$

Based thereon, the regularized crack surface can be defined as

$$\Gamma_l(d) = \int_{\Omega} \gamma(d, \nabla d) \, dV. \quad (15)$$

In this equation, γ is the crack density and Ω denotes the physical domain of the body. [47] proposed γ to consist of two terms, a polynomial and a gradient term, i.e.,

$$\gamma(d) = \frac{1}{2l_f} d^2 + \frac{1}{2} l_f |\nabla d|^2, \quad (16)$$

where l_f is a positive constant describing an internal length scale. The expression γ represents therefore an approximation of a sharp crack surface density. For the vanishing length scale $l_f \rightarrow 0$, the regularized interface reduces to a sharp one. According to [47], the damage parameter is then said to minimize the regularized crack surface, which results in the Euler–Lagrange equations

$$d - l_f^2 \Delta d = 0 \quad \text{in } \Omega \quad \text{and} \quad \nabla d \cdot \mathbf{n}_0 = 0 \quad \text{on } \partial_{n_0} \Omega \quad (17)$$

under the Dirichlet boundary condition $d(\mathbf{X}, t) = 1$ on $\mathbf{X} \in \Gamma_l(t)$; \mathbf{n}_0 denotes the outwards normal on the surface. It is required that the minimizer of the regularized smooth functional Γ_l converges to the minimizer of the functional Γ in the limiting case $l \rightarrow 0$. Furthermore, the minimizers have to be local and stable in the presence of continuous perturbations [11], where the perturbations are controlled by the higher-order term ∇d . However, Maqy et al. [45] have proven numerically that Γ -convergence is not necessarily obtained for the discretized formulation for brittle fracture based on the functional in equation (16). This is addressed by Linse et al. [42] to root from the irreversibility condition, which results in a high amount of error in the approximated crack surface energy. Bourdin [10] considered the phase-field parameter to be locally reversible. That means the phase-field parameter could decrease locally at some points while increasing at others. Furthermore, within his approach, the Dirichlet-type boundary conditions are enforced as soon as the phase-field parameter reaches the value $d = 1$. In other words, the crack can not heal as soon as it is formed.

The model of Miehe et al. [47] incorporated local irreversibility of the phase-field parameter. Later on, Miehe et al. [50] enforced this local constraint just in a specified part of the domain. This region was defined as material points reaching a certain amount of energy. This approach will be discussed in more detail in section 3.1 as it will be in close connection to the local reversibility feature of our model. For more technical details regarding phase-field modeling of brittle fracture in line with the approach of Miehe et al. [47] see Appendix B.

3 An extended phase-field fracture approach

In this section, we first briefly summarize the main approaches in the literature to address the issue of irreversibility and associated Γ -convergence in Sect. 3.1 in order to motivate our extension proposed in Sect. 3.2, which is followed by a further micromorphic extension for the ductile aspect in Sect. 3.3 and a description of a potential algorithmic implementation in Sect. 3.4.

3.1 Γ -convergence and irreversibility constraints of existing phase-field fracture formulations

In the context of the approach proposed in this paper, the connected notions of Γ -convergence and thermodynamical consistency will be particularly important. Therefore, we first discuss existing formulations with view to these aspects. Thermodynamic consistency is discussed in the sense that the total amount of dissipated energy in the body should not reduce over time, i.e., no healing should occur. Most existing formulations consider a *local irreversibility*, i.e., the damage parameter d at the material point is not allowed to decrease over time. This automatically ensures that also the dissipation rate is always positive at every material point and thus, also over the total body. However, the damage parameter d in phase-field fracture formulations is rather an auxiliary variable to describe a diffuse crack. It does not necessarily phenomenologically describe a softening response resulting from micro-cracks or -voids in the bulk material, which would be the physical basis for continuum damage mechanics models. Thus, in continuum damage mechanics, it is indeed physically required that the damage variable does not decrease over time. For phase-field fracture, however, it means that a locally irreversible evolution of the auxiliary parameter d is not essential. In fact, it may be sufficient to only ensure that \dot{d} stays positive if d reaches the value one, i.e., whenever it describes the physical crack. Everywhere else, \dot{d} may be allowed to be negative, provided that the associated dissipation rate remains non-negative. This behavior will be referred to as *crack irreversibility* in this paper. There are even possible physical explanations for such a response, considering that the microstructural effects at the crack happen at a very small scale. For instance, the intrinsic nonlinearity due to the anharmonicity of potentials associated with atomic binding forces [55] may explain a nonlinear elastic unloading, which occurs close to the crack upon complete detachment of the neighboring crack surfaces. This corresponds to a decrease in d but no decrease in local dissipation, which may only happen for small values of d . This important difference between phase-field fracture and continuum damage mechanics will be significant to the model proposed in this paper. In the context of the issues of irreversibility and Γ -convergence, already existing formulations can be mainly categorized into the following four groups.

3.1.1 Models without irreversibility constraint

Karma et al. [32] and Hamkin and Karma [25] considered a double-well potential to define the crack surface energy. However, a non-convex degradation function was introduced in their formulation, which does not fulfill the crack irreversibility of an initiated crack [49]. The approach proposed here will, however, make use of the double-well potential in combination with the modified degradation function given in (28).

3.1.2 Locally reversible phase-field parameter accompanied by a global constraint

Bourdin [10] introduced a formulation that allows the local reversibility of the phase-field parameter. That means, the phase-field parameter can increase as well as decrease, and no restriction is taken into consideration. This approach enforces the crack irreversibility of the phase-field parameter as soon as it reaches the value one by adaptively incorporating a special Dirichlet-type boundary condition. Although this model is reported to be Γ -convergent, it is not in general thermodynamically consistent [50].

3.1.3 Locally irreversible phase-field parameter accompanied by a fracture threshold

The third group is based on the work of Miehe et al. [47], where similar to continuum damage formulations, a fracture threshold is determined. This threshold is mainly based on the local fracture driving force, where the negative driving forces are neglected. Additionally, to fulfill thermodynamic consistency, a local irreversibility condition is enforced. This constraint prohibits the negative evolution of the phase-field parameter. This type of formulation is used to model fracture in elastic–plastic solids by different authors. For instance, Duda et al.

[17] studied brittle fracture in elasto-plastic solids. In their work, only the degradation of the elastic energy is taken into consideration, and the plastic energy remains untouched in the fully broken medium. Based on this assumption, the total energy per unit volume at time t_{n+1} has the form

$$w = g(d)\psi_0^e(\mathbf{C}^e) + \psi^p(\alpha) + g_c\gamma(d, \nabla d). \quad (18)$$

Following this assumption, the plastic energy has no contribution to the local driving force acting on the crack tip. In other words, the crack propagates in the region with the highest elastic energy. However, in e.g., ductile metals, a classical observation is that shear bands are formed prior to crack propagation. Hence, one can conclude that ignoring the degradation of plastic energy could be an acceptable assumption just in case of brittle fracture. Ambati et al. [5] and Ambati et al. [6] proposed a modified degradation function consisting of both, damage parameter d and accumulative plastic strain α . This type of modification is offered to postpone the phase-field parameter's evolution to take place after a certain amount of plastic work. However, this assumption makes the stress-like internal variable defined in equation (62) to be dependent on the elastic energy which is physically questionable. On the other hand, Kuhn et al. [37] and Borden et al. [9] considered both, elastic and plastic energies to degrade. Based on this assumption, the total energy per unit volume has the form

$$w = g(d)(\psi_0^e(\mathbf{C}^e) + \psi_0^p(\alpha)) + g_c\gamma(d, \nabla d). \quad (19)$$

where in Kuhn et al. [37], a higher-order degradation function is used. Although being thermodynamically consistent, such kinds of formulations have been numerically shown not to be Γ -convergent [45]. One reason for the lack of Γ -convergence in this type of formulations is the enforcement of local irreversibility [50].

3.1.4 Locally irreversible phase-field parameter accompanied by a modified fracture threshold

The fourth group of formulations is a modified version of the third group, see Miehe et al. [50]. Using this modification, the total energy per unit volume has the form

$$w = g(d)(\psi_0^e(\mathbf{C}^e) + \psi_0^p(\alpha)) + (1 - g(d))w_c + 2w_c l_f \gamma(d, \nabla d), \quad (20)$$

where w_c is the constant crack threshold parameter. This results in a non-zero energy $w = 2w_c$ in the case of fully broken material. However, this modification enables to postpone the evolution of phase-field parameter to take place after a certain amount of energy is reached. Furthermore, a local irreversibility constraint is considered, which does not allow the local reduction of the phase-field parameter. This means that the phase-field parameter would only evolve in the region, where the minimum energy threshold is reached and the irreversibility is enforced within this region. Although this modification bounds the irreversibility of the phase-field parameter to a specific localized region, the issue attributed to the enforcement of local irreversibility is not resolved completely and is just reduced to a smaller scale. In case that more localization has taken place within this region, this results in a sharper gradient of the phase-field parameter and, consequently, a higher micromechanical stress vector \mathbf{Y} . However, the presence of the local irreversibility constraint would result in an under-approximated micromechanical stress vector. Moreover, to the best of our knowledge, discretized forms of this modification have not been proven to be Γ -convergent.

3.2 Proposed phase-field formulation

In this section, a modified phase-field fracture approach is proposed. Whereas classical approaches define the crack surface as a singular surface, in this framework, the crack surface is defined as a volumetric domain where $0 < d < 1$. Actually, this approach reflects the fact that a crack is not a macroscopic singular surface in reality which is due to the microstructure, leading to complex patterns in the crack neighborhood. Therefore, it is more in line with the basic conception of phase-field approaches, since the crack is described as diffuse interface. In fact, it appears only natural to also consider the crack surface, i.e., where $d = 1$, as a diffuse zone. Furthermore, in contrast to the by now classical phase-field fracture approaches, where the local damage parameter can only increase, in the proposed modification the phase-field parameter is considered to smear a crack rather than describing a continuous degradation of the material. Therefore, the phase-field parameter is locally assumed to be able to do both, increase or decrease, before it reaches the value $d = 1.0$. Of course, the crack shall not be allowed to heal and thus, the phase-field parameter shall not reduce at points where d has reached the value. This is addressed later on by an a priori global irreversibility in the sense that global

dissipation will not have negative evolution. This can be interpreted as a pure phase-transformation, where a fully intact phase with density $\rho = \rho_0$ could transform to a fully cracked phase with zero mass and therefore zero density $\rho = 0$. This motivates the definition of the phase-field parameter using the mass density, similar to the theory of mixtures

$$d = \frac{\rho_0 - \rho}{\rho_0} \quad \text{with} \quad 0 < \rho \leq \rho_0. \quad (21)$$

where ρ_0 denotes the mass density of the intact material and ρ corresponds to the mass density in the diffuse crack. For the limit of a sharp crack, the phase-field parameter can be defined using a step function

$$d = \begin{cases} 0 & \text{for } \rho = \rho_0 \text{ (fully intact),} \\ 1 & \text{for } \rho = 0 \text{ (fully cracked).} \end{cases} \quad (22)$$

Here, it is even physically meaningful to state that $\rho = 0$ for the fully cracked scenario corresponds to a realistic state, since $d = 1$ is allowed in a volumetric domain and mass density is only defined on a volume. The values between zero and one characterize the diffuse region in between; $d = 1$ represents the crack surface in a smeared sense. Motivated thereby, we define the spatial distribution of the damage parameter to follow the tangent hyperbolic function

$$d(x) = \frac{1}{2} \left(1 + \tanh \left(\frac{x - x_0}{l_f} \right) \right), \quad (23)$$

where according to the Allen–Cahn theory, the crack surface is the diffuse interface between fully intact and fully broken phases, as depicted for the 1D case in Fig. 1a. This distribution can be obtained as minimizer of the crack surface

$$\Gamma_{l_f}(d) = \int_{-\infty}^{\infty} \frac{6}{l_f} d^2 (1 - d)^2 + \frac{3}{2} l_f |\partial_x d|^2 dX, \quad (24)$$

where x_0 is the position of the crack interface. Note that this functional has already been proposed in Mosler et al. [53] for the description of homogenized two-phase materials. It represents a rescaled form of the Modica–Mortola-type functional proposed by [11], see also [52], which has been shown to be Γ -convergent. Extending this crack surface to the three-dimensional setting following [53] and considering the Griffith constant g_c , the crack surface energy reads

$$D_{l_f}(d) = \int_{\Omega} g_c \gamma(d, \nabla d) dV \quad \text{with} \quad \gamma(d, \nabla d) = \frac{6}{l_f} d^2 (1 - d)^2 + \frac{3}{2} l_f |\nabla d|^2 \quad (25)$$

Here the positive constant l_f is the length scale of the crack surface that regularizes a sharp crack into a smeared one. In contrast to the definition of the crack surface energy following [47] (see (72) in Appendix A), this functional is based on a double-well potential. Similar to continuum damage mechanics, we consider the degradation function initially introduced in [47] as

$$g(d) = (1 - d)^2, \quad (26)$$

which has the properties

$$g(d) \geq 0 \quad \text{with} \quad g(1) = g'(1) = 0, \quad g(0) = 1. \quad (27)$$

The first equality in equation (27) is obtained from the fact that in the fully damaged material, both the stored energy and the thermodynamic force are zero. In order to avoid numerical instabilities associated with ill-conditioned boundary value problems resulting from $d = 1$, a residual energy per unit volume is often considered to remain in the fully cracked material point. This residual energy density is said to be a small portion of the strain energy density in the intact zone, that is $\psi_{ex} = \varepsilon \psi_0$, where $0 < \varepsilon \ll 1$ is a positive constant. Miehe et al. [47] considered this parameter to be present for all values of d and consequently, the degradation function is modified as

$$g_{\text{MWH}}^{\text{mod}}(d) = g(d) + \varepsilon. \quad (28)$$

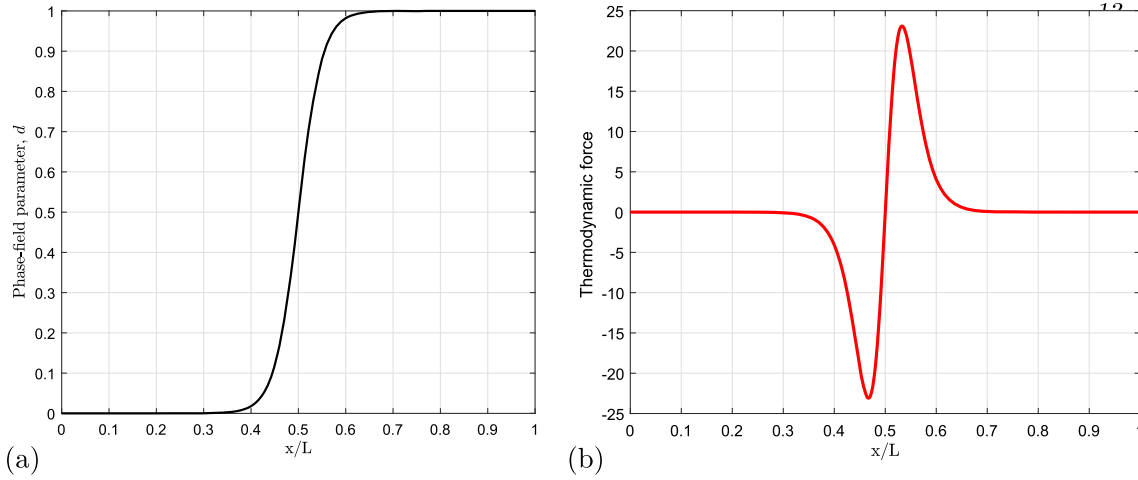


Fig. 1 Distribution of **a** phase-field parameter d and **b** part of the micromechanical internal force (second additive term on the right-hand side of (39)) over a one-dimensional bar with $l_f = 0.05$, $x_0 = 0.5L$

Some other authors have defined the residual energy not to be present everywhere, i.e., not when the material is intact. Therefore, Spetz et al. [65] used the definition $g_{\text{SDTD}}^{\text{mod}}(d) = \varepsilon + g(d)(1 - \varepsilon)$. However, these types of degradation functions results in a loss of stiffness before fracture occurs, which is not desirable for the modeling of fracture in brittle materials. Hence, for such materials Kuhn et al. [36] introduced a multi-well degradation function. Although this type of degradation function will diminish the stiffness loss before the crack nucleation, it results in more admissible solutions. Therefore, on top of that, a numerical perturbation is introduced. However, the effect of such a numerical treatment on the quality of solution is not well studied. Hence, we build our model based on the degradation function proposed in (28).

Using the quadratic degradation function and applying it to the bulk strain energy density [9,37], the total energy density is given as

$$w = g(d)(\psi_0^e(\mathbf{C}^e) + \psi_0^p(\alpha)) + d^2(1 - d)^2 \frac{\psi_{cr}^p}{l_f} + g_c \gamma(d, \nabla d), \quad (29)$$

where ψ_0^e is the fictitiously undamaged, elastic part of the strain energy density depending on the elastic part of the right Cauchy-Green tensor \mathbf{C}^e , and ψ_0^p is the fictitiously undamaged plastic part associated to hardening which depends on the accumulated plastic strains α . For details regarding the specific elasto-plastic formulation considered in this paper see Appendix A. In the context of ductile crack propagation, usually plastic shear bands form prior to the crack. In order to postpone the crack evolution to only happen for higher values of plastic energy, the additional term $d^2(1 - d)^2 \psi_{cr}^p / l_f$ is added. Herein, ψ_{cr}^p is a material parameter representing a threshold associated with the plastic energy. The additional term is chosen such that it does not modify the energy density whenever $d = 0$ and $d = 1$. However, if $\frac{\psi_{cr}^p}{l_f}$ is much greater than g_c , which may physically be required, the gradient regularization term becomes insignificant. Therefore, the plastic energy threshold is additionally multiplied with the gradient term rescaled by a factor of 1/4, i.e.,

$$w = g(d)(\psi_0^e(\mathbf{C}^e) + \psi_0^p(\alpha)) + \frac{\psi_{cr}^p}{l_f} [d^2(1 - d)^2 + \frac{1}{4} l_f^2 |\nabla d|^2] + g_c \gamma(d, \nabla d). \quad (30)$$

Taking this modification into account, the equation (30) reduces to

$$w = g(d)(\psi_0^e(\mathbf{C}^e) + \psi_0^p(\alpha)) + (g_c + \psi_{cr}^p/6) \gamma(d, \nabla d), \quad (31)$$

which is in line with Irwin's approach (1) for ductile fracture. Note that this energy density vanishes in the domain of the smeared crack, i.e., whenever $d = 1$, and we obtain the physically reasonable limiting cases

$$w = \begin{cases} \psi_0^e + \psi_0^p & \text{if } d = 0, \\ 0, & \text{if } d = 1, \end{cases} \quad (32)$$

except for the points infinitely close to the interface $0 < d < 1$. Furthermore, the damage parameter does not affect the yield function defined in equation (63) due to applying the degradation to both, ψ_0^e and ψ_0^p .

The micromechanical internal force in line with the Allen–Cahn theory is obtained as the driving force conjugated to \dot{d} , i.e.,

$$-\frac{\partial w}{\partial d} = 2(1-d) \left(\psi_0^e(\mathbf{C}^e) + \psi_0^p(\alpha) \right) - \frac{12}{l_f} (g_c + \psi_{cr}^p/6) \left[2d^3 - 3d^2 + d \right]. \quad (33)$$

Therefore, the micromechanical internal force vanishes automatically for the fully damaged and the unloaded intact case, i.e.,

$$-\frac{\partial w}{\partial d} = \begin{cases} 0 & \text{if } d = 0 \wedge \psi_0^e = \psi_0^p = 0, \\ 0 & \text{if } d = 1, \end{cases} \quad (34)$$

and no special treatment in terms of additional case distinctions is required. Furthermore, in contrast to the classical approaches as discussed in Sect. 3.1.3, one could reasonably erode the elements in the fully cracked region with $d = 1.0$ since the energy stored there as well as the driving force are zero. The micromechanical stress vector conjugate to $\nabla \dot{d}$ reads

$$\boldsymbol{\Upsilon} = \frac{\partial w}{\partial \nabla d} = 3(g_c + \psi_{cr}^p/6) l_f \nabla d. \quad (35)$$

Fulfilling the dissipation inequality requires that the dissipation becomes zero if local reversibility is allowed. Therefore, we consider the split of the dissipation inequality

$$\mathcal{D}^f = \frac{1}{2} \left[\kappa \left(\frac{|\dot{d}| + \dot{d}}{2} \right)^2 + \eta \left(\frac{\dot{d} - |\dot{d}|}{2} \right)^2 \right] \geq 0, \quad (36)$$

for $\kappa \geq 0$ and $\eta \geq 0$. This dissipation is identical to (11) if $\eta = \kappa$. Remember that κ is the interface mobility parameter which controls the evolution rate of the phase-field parameter. The split allows to specifically address a separate parameter η to the case where $\dot{d} < 0$. However, here, we assume that the local reversibility should not produce dissipation, cf. Sect. 3.1, and thus, η is set to zero and the dissipation inequality reads

$$\mathcal{D}^f = \frac{1}{2} \kappa \langle \dot{d} \rangle^2, \quad (37)$$

with the Macauley brackets defined as $\langle (\bullet) \rangle := (|\bullet| + \bullet)/2$. Following the balance of micromechanical forces (12) in the absence of external forces, and $\partial_i \mathcal{D}^f = \kappa \langle \dot{d} \rangle$, the Allen–Cahn-type equation can be obtained

$$\kappa \langle \dot{d} \rangle = -\frac{\partial w}{\partial d} + \nabla \cdot \boldsymbol{\Upsilon}. \quad (38)$$

Note that this evolution equation is identical to the classical balance of micro-forces in the context of the Allen–Cahn or time-dependent Ginzburg–Landau theory if the Macauley brackets are omitted, see (12) and (13). The small difference in terms of the Macauley brackets, already included in the definition of the dissipation (37), is however physically important. Since the original theory is meant for phase transformations, where a negative evolution of the phase-field parameter results in positive change of dissipation, omitting the Macauley bracket is actually physical since phases can transform back upon further dissipation. In case of our fracture model, where the phase-field parameter is only meant to regularize a sharp crack, not to describe stress-softening, this is different. Then a negative evolution of the phase-field parameter is locally allowed, however, no dissipation should be produced. By a direct comparison with the original formulation (12), one can see that the left-hand side in (38) vanishes, which could be reached in the original framework by setting the mobility κ to zero. This dependence on \dot{d} is automatically included here. This equation can be solved as additional partial differential equation using the finite element method to obtain the distribution of the damage parameter. One major difference with the preexisting models by Bourdin [10], Miehe et al. [47] and Miehe et al. [50] is the fact that neither local nor crack irreversibility constraint is needed. This can be shown by considering a one-dimensional problem. Let us consider a bar fully cracked on the right-hand side and fully intact on the left

side. According to equation (23), the phase-field parameter is distributed according to a tangent-hyperbolic-type function depicted in Fig. 1a. Replacing the phase-field parameter into the equations of micromechanical internal force and stress in Eqs. (33) and (35), respectively, the right-hand side of equation (38) is obtained as

$$\kappa \langle \dot{d} \rangle = -\frac{\partial w}{\partial d} + \nabla \cdot \Upsilon = 2(1-d) \left(\psi_0^c(\mathbf{C}^c) + \psi_0^p(\alpha) \right) - \frac{6}{l_f} (g_c + \psi_{cr}^p/6) [2d^3 - 3d^2 + d]. \quad (39)$$

The first additive term in the right-hand side of this equation is always non-negative. The resultant of the micromechanical force according to the second additive term acting on the whole interface reads

$$t = \frac{6}{l_f} (g_c + \psi_{cr}^p/6) \int_0^L (2d^3 - 3d^2 + d) dX = 0 \quad (40)$$

and always vanishes due to the point symmetry of the distribution, in this context see also Fig. 1b. Therefore, only the first additive term influences the evolution of the crack. In the specific example considered here, where the crack exists on the right-hand side of the bar, the non-negativity of the first additive term results in a micromechanical force acting on the interface which pushes the interface from right to left, not vice versa. That is, the intact phase with the phase-field parameter $d = 0$ could only transform to the cracked phase with the phase-field parameter $d = 1$. This shows that crack irreversibility is automatically fulfilled and hence, the lack of Γ -convergence associated with irreversibility constraints is a priori removed using the proposed formulation. Furthermore, it is necessary to emphasize, that the phase-field parameter is between zero and one only at the interface between fully intact and cracked domains and away from the interface it is either zero or one.

3.3 Micromorphic extension for ductile fracture

The evolution of accumulative plastic strains could result in localized shear bands, which would have a strong impact on the subsequent crack propagation process in case of ductile fracture. In order to overcome the numerical difficulties associated with the localization, micromorphic approaches have been developed. The main idea there is the coupling of an additional global field to the local field via a length scale parameter and the gradient of the new global field. Thereby, this approach shares structural similarities with phase-field formulations. However, major difference can be seen in the micromechanical origin in the physics behind the two approaches yielding different energy potentials. The concept of adding additional degrees of freedom, representing the effects of microstructure on the macroscopic deformation, goes back to the 1960s, cf. [18,51]. The micromorphic setting in the general sense has been proposed in Forest [19]. The micromorphic theory originates from Eringen's definition of a microdeformation tensor, where it is extended to other global variables such as the accumulative plastic strains α [19].

Although in the proposed formulation in Sect. 3.2, the material length scale l_f , the gradient of damage parameter, and the viscosity term for the evolution of the phase-field variable are incorporated, there exists no direct control of the evolution of the accumulative plastic strains to prevent localization. This would be important, if the damage evolution starts after a higher amount of plastic work has taken place as it is the case in ductile materials. Hence, the implementation of ductile fracture formulation proposed in this paper is extended here by considering a new nonlocal plastic variable $\tilde{\alpha}$ which can be interpreted as accumulative plastic micro-strain. Therefore, the following micromorphic plastic energy density term $\tilde{\psi}_0^p(\alpha, \tilde{\alpha}, \nabla \tilde{\alpha})$ is added to the plastic energy density defined in (67). This additional energy considers a quadratic term which connects the local and nonlocal variables and a term which is quadratic in the gradients of the nonlocal variable. The additional energy density reads

$$\tilde{\psi}_0^p(\alpha, \tilde{\alpha}) = \frac{\chi}{2l_p} (\alpha - \tilde{\alpha})^2 + \chi l_p \nabla \tilde{\alpha} \cdot \nabla \tilde{\alpha}, \quad (41)$$

cf. [19] and [16], wherein, χ and l_p are material constants. Since the micromorphic energy should also be influenced by the evolution of damage, it is multiplied with the degradation function. In other words, the fictitious micromorphic energy will also degrade as the phase-field parameter grows. Therefore, equation (31) is modified as

$$w = g(d)(\psi_0^c(\mathbf{C}^c) + \psi_0^p(\alpha) + \tilde{\psi}_0^p(\alpha, \tilde{\alpha}, \nabla \tilde{\alpha})) + (g_c + \psi_{cr}^p/6)\gamma(d, \nabla d), \quad (42)$$

and the micromechanical internal force in equation (33) reads

$$-\frac{\partial w}{\partial d} = 2(1-d) \left(\psi_0^e(\mathbf{C}^e) + \psi_0^p(\alpha) + \tilde{\psi}_0^p(\alpha, \tilde{\alpha}, \nabla \tilde{\alpha}) \right) - \frac{12}{l_f} (g_c + \psi_{cr}^p/6) \left[2d^3 - 3d^2 + d \right]. \quad (43)$$

Note that although the micromechanical stress vector remains unchanged, the micromechanical internal force is affected by the fictitious micromorphic energy. Moreover, the thermodynamic force associated to the accumulative plastic strain in equation (62) is rewritten as

$$Q := \frac{\partial \psi_0}{\partial \alpha} = \frac{\partial \psi_0^p(\alpha) + \tilde{\psi}_0^p(\alpha, \tilde{\alpha}, \nabla \tilde{\alpha})}{\partial \alpha} = \frac{\partial \psi_0^p(\alpha)}{\partial \alpha} + \frac{\chi}{l_p} (\alpha - \tilde{\alpha}), \quad (44)$$

where the term $\frac{\chi}{l_p}$ can be interpreted as the size-dependent linear isotropic hardening modulus. This extra term affects also the plastic yield condition and thus, the overall plastic response. As a consequence of that, the plastic zone, which would have been prone to localization for the unregularized model, will become more diffuse but mesh-independent.

3.4 Algorithmic implementation

In order to solve a boundary value problem using the proposed formulation in this paper, the rate-type variational principle is used, that is to find the minima of the function (76), accompanied by a local maximization. In this setting, the global fields are the rates of deformation mapping φ , phase-field parameter d and the micromorphic variable $\tilde{\alpha}$. To obtain the discretized form of the formulation proposed in this paper, during which the internal and state variables evolve with time, the incremental variational setting must be developed. This incremental setting is given in the time interval $[0, T]$ such that the discrete time step τ_{n+1} is introduced as

$$\tau_{n+1} = t_{n+1} - t_n > 0. \quad (45)$$

Each state variable is considered at each discrete time point $0, t_1, t_2, \dots, t_n, t_{n+1}, \dots, T$. Furthermore, the field variables are assumed to be known at time t_n . In general, the incremental form of the rate of stored energy, external power and dissipation are obtained as

$$\mathcal{E}^{\text{inc}}(\varphi, d) = \int_{\Omega} [\psi_{n+1}(\mathbf{F}_{n+1}, d_{n+1}, \tilde{\alpha}_{n+1}) - \psi_n(\mathbf{F}_n, d_n, \tilde{\alpha}_n)] dV =: E_{n+1} - E_n, \quad (46)$$

where E_{n+1} and E_n are the values of the stored energy at time t_{n+1} and t_n , respectively. Furthermore, the global field $\tilde{\alpha}$ is coupled to the local field α . The plastic deformation gradient and the accumulative plastic strain are computed locally at each Gauß integration point and the elastic deformation gradient and the elasto-plastic tangent \mathbb{C}_0^{ep} are updated. That is, for each Newton iteration at each Gauß-integration point the yield condition is checked and if the admissible domain $\phi \leq 0$ is not fulfilled, then the evolution equation (64) together with $\phi = 0$ are solved, where the evolution equation is discretized using the implicit backward Euler integration scheme

$$\mathbf{F}_{n+1}^p := \mathbf{F}_n^p + \Delta\lambda \mathbf{N}_{n+1} \cdot \mathbf{F}_{n+1}^p. \quad (47)$$

This results in a system of ten equations and ten unknowns (the components of plastic deformation gradient at time t_{n+1} and the increment of plastic multiplier $\Delta\lambda$), which is solved iteratively and based on that, the accumulative plastic strain at time t_{n+1} is obtained as

$$\alpha_{n+1} = \alpha_n + \Delta\lambda. \quad (48)$$

The incremental form of external power is derived in analogy to (46) as

$$\mathcal{P}^{\text{inc}}(\varphi) := \int_{t_n}^{t_{n+1}} \dot{\mathcal{P}} dt = \int_{\Omega} \rho_0 \mathbf{b} \cdot (\varphi_{n+1} - \varphi_n) dV + \int_{\partial\Omega} \mathbf{T} \cdot (\varphi_{n+1} - \varphi_n) dA. \quad (49)$$

The general incremental form of a dissipation functional is obtained as

$$\mathcal{D}^{\text{inc}}(d) = \int_{\Omega} [\gamma_{n+1}(d_{n+1}, \nabla d_{n+1}) - \gamma_n(d_n, \nabla d_n)] \, dV. \quad (50)$$

Finally, the incremental total potential energy can be written as

$$\mathcal{W}^{\text{inc}}(\boldsymbol{\varphi}, d, \tilde{\alpha}) = \mathcal{E}^{\text{inc}}(\boldsymbol{\varphi}, d, \tilde{\alpha}) + \mathcal{D}^{\text{inc}}(d) - \mathcal{P}^{\text{inc}}(\boldsymbol{\varphi}), \quad (51)$$

whose infimum is sought in each time step with respect to the primary variables which include the deformations $\boldsymbol{\varphi}$, the damage phase-field parameter d as well as the nonlocal accumulated plastic strains $\tilde{\alpha}$. For this purpose, the first variation with respect to d_{n+1} , \mathbf{F}_{n+1} and $\tilde{\alpha}_{n+1}$ is computed as

$$\delta_{(\mathbf{F}, d, \tilde{\alpha})} \mathcal{W}^{\text{inc}} = \frac{\partial \mathcal{W}^{\text{inc}}}{\partial \mathbf{F}} : \delta \mathbf{F} + \frac{\partial \mathcal{W}^{\text{inc}}}{\partial d} \delta d + \frac{\partial \mathcal{W}^{\text{inc}}}{\partial \tilde{\alpha}} \delta \tilde{\alpha} = 0, \quad (52)$$

where, for the sake of simplicity, the subscript $n + 1$ is dropped. For the solution of this nonlinear equation, the Newton–Raphson scheme is used here. For this purpose, the linearization of (52) results in the linear increment

$$\begin{aligned} \Delta_{(\mathbf{F}, d, \tilde{\alpha})} \delta_{(\mathbf{F}, d, \tilde{\alpha})} \mathcal{W}^{\text{inc}} &= \Delta \mathbf{F} : \frac{\partial^2 \mathcal{W}^{\text{inc}}}{\partial \mathbf{F} \partial \mathbf{F}} : \delta \mathbf{F} + \Delta d \frac{\partial^2 \mathcal{W}^{\text{inc}}}{\partial d^2} \delta d + \Delta \tilde{\alpha} \frac{\partial^2 \mathcal{E}^{\text{inc}}}{\partial \tilde{\alpha}^2} \delta \tilde{\alpha} \\ &+ \Delta d \frac{\partial^2 \mathcal{E}^{\text{inc}}}{\partial d \partial \tilde{\alpha}} \delta \tilde{\alpha} + \Delta d \frac{\partial^2 \mathcal{E}^{\text{inc}}}{\partial d \partial \mathbf{F}} : \delta \mathbf{F} + \Delta \mathbf{F} : \frac{\partial^2 \mathcal{E}^{\text{inc}}}{\partial \mathbf{F} \partial \tilde{\alpha}} \delta \tilde{\alpha} \\ &+ \Delta \tilde{\alpha} \frac{\partial^2 \mathcal{E}^{\text{inc}}}{\partial d \partial \tilde{\alpha}} \delta d + \Delta \mathbf{F} : \frac{\partial^2 \mathcal{E}^{\text{inc}}}{\partial d \partial \mathbf{F}} \delta d + \Delta \tilde{\alpha} \frac{\partial^2 \mathcal{E}^{\text{inc}}}{\partial \mathbf{F} \partial \tilde{\alpha}} : \delta \mathbf{F}. \end{aligned} \quad (53)$$

The linearized equation $\delta_{(\mathbf{F}, d, \tilde{\alpha})} \mathcal{W}^{\text{inc}} + \Delta_{(\mathbf{F}, d, \tilde{\alpha})} \delta_{(\mathbf{F}, d, \tilde{\alpha})} \mathcal{W}^{\text{inc}} = 0$ is here solved using finite elements with a linear approximation of the primary variables. The increments and variations of the deformation gradients $\Delta \mathbf{F}$ and $\delta \mathbf{F}$, are computed from the associated increments and variations of the deformations $\Delta \boldsymbol{\varphi}$ and $\delta \boldsymbol{\varphi}$, respectively. Considering arbitrary values for the variations of the primary variables and assembling over all finite elements yields the system of equations

$$\begin{bmatrix} \mathbf{K}_{\varphi\varphi} & \mathbf{K}_{\varphi d} & \mathbf{K}_{\varphi\tilde{\alpha}} \\ \mathbf{K}_{d\varphi} & \mathbf{K}_{dd} & \mathbf{K}_{d\tilde{\alpha}} \\ \mathbf{K}_{\tilde{\alpha}\varphi} & \mathbf{K}_{\tilde{\alpha}d} & \mathbf{K}_{\tilde{\alpha}\tilde{\alpha}} \end{bmatrix} \begin{bmatrix} \Delta \mathbf{D}_{\varphi} \\ \Delta \mathbf{D}_d \\ \Delta \mathbf{D}_{\tilde{\alpha}} \end{bmatrix} = \begin{bmatrix} \mathbf{R}_{\varphi} \\ \mathbf{R}_d \\ \mathbf{R}_{\tilde{\alpha}} \end{bmatrix}, \quad (54)$$

which has to be solved within each Newton step to obtain the updated solution until a predefined tolerance in terms of the norm of the linear increment is reached. The individual terms of the stiffness matrix \mathbf{K} and the residual vector \mathbf{R} are obtained from the individual terms in the linearized equation in the classical manner. For instance, when considering the approximation for the deformations leading to the approximated form of the deformation gradients written in matrix form as $\delta \mathbf{F} = \mathbf{B}^e \mathbf{d}_{\varphi}^e$ with the well-known B-matrix \mathbf{B}_e including the derivatives of the shape functions and the element-wise vector of deformation degrees of freedom \mathbf{d}_{φ}^e , the first term in (53) yields the term $\delta \mathbf{d}_{\varphi}^{eT} \mathbf{k}_{\varphi\varphi}^e \Delta \mathbf{d}_{\varphi}^e$ with the element stiffness matrix $\mathbf{k}_{\varphi\varphi}^e = \int_{\Omega^e} \mathbf{B}_e^T \mathbf{g}(d) \mathbb{C}^{\text{ep}} \mathbf{B}_e \, dV$. Assembling $\mathbf{k}_{\varphi\varphi}^e$ and $\Delta \mathbf{d}_{\varphi}^e$ in global counterparts yields the entries in $\mathbf{K}_{\varphi\varphi}$ and $\Delta \mathbf{D}_{\varphi}$, respectively. All other terms in (53) are reformulated in matrix form accordingly to obtain the coupled system of equations (54). This strategy has been implemented in ABAQUS/Standard [1] and based thereon, the boundary value problems analyzed in the following section are solved using a monolithic scheme. The evolution equations are integrated using backward Euler in a multilevel Newton context. For the phase field and the micromorphic field purely zero Neumann conditions are defined at the boundary.

Remark To solve the phase-field fracture problem governing an incremental setting, some authors have used a one-pass operator-splitting algorithm, cf. Aldakheel et al. [2], Gültekin et al. [22,23], Spetz et al. [65], Miehe et al. [48], Ambati et al. [6], Proserpio et al. [59]. The splitting algorithm reduces the problem into a decoupled one. However, considering a dissipation inequality enables the monolithic solution of the coupled problem. The dissipation inequality is discussed in Sects. 2 and 3.2.

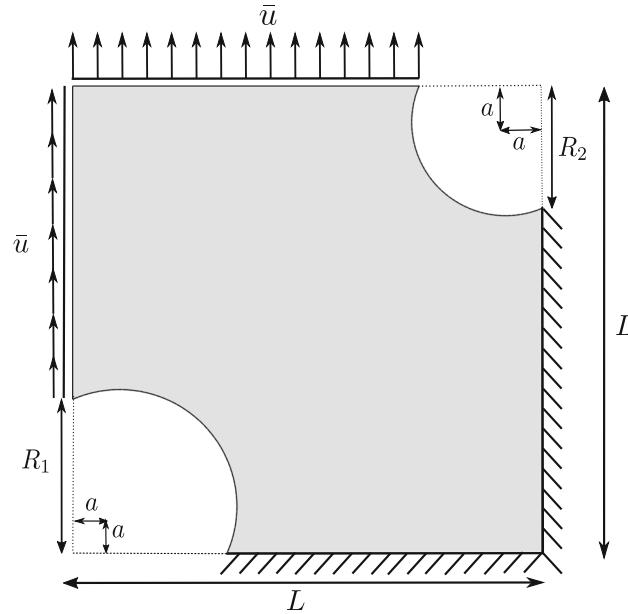


Fig. 2 The geometry and boundary conditions of the double-notched specimen

Table 1 Geometrical dimensions of the unsymmetrical double-notched specimen depicted in Fig. 2

Geometrical parameter	Value in mm
L	10
t	0.3
R_1	2.5
R_2	2.0
a	1.0

4 Simulation and results

To show the efficiency and numerical robustness of the proposed formulation, FE simulations for two benchmark problems are performed and the results are discussed in detail. The modified model is implemented in ABAQUS, defining the phase-field parameter as the fourth degree of freedom in a three-dimensional 8-node element via a user element subroutine (UEL). The problems are solved fully coupled and monolithically using the multilevel Newton–Raphson method and automatic adaptive load stepping.

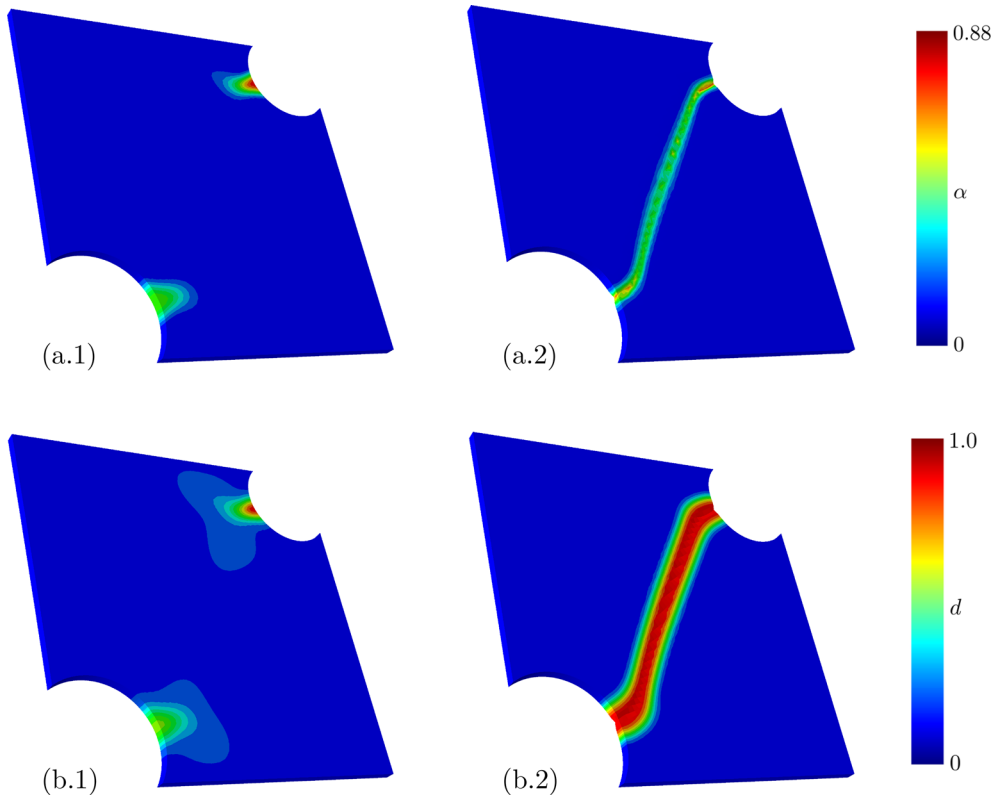
4.1 Tensile test of an unsymmetric double-notched specimen

In the first analysis, a three-dimensional unsymmetric double-notched specimen is chosen, subject to the displacement $\bar{u} = 0.152$ mm at the top and left surfaces, which are applied in 317 load steps. The bottom and right surfaces are clamped. An illustration of the boundary value problem is given in Fig. 2 and the geometrical dimensions of the specimen are given in Table 1. A number of 6032 finite elements is used for the discretization of the specimen. The characteristic element length h_e is chosen to be $h_e < l_f/2$ in the whole region, where the crack is expected to form and propagate. The numerical analysis is performed using the material parameters given in Table 2.

It is observed that the accumulative plastic strains get localized at the notches, cf. Figure 3a.1. As a consequence, the phase-field parameter also gets localized and forms a crack path within those regions as shown in Fig. 3b. The final crack path as shown in Fig. 3b.2 is qualitatively very close to the results provided in Seupel et al. [63], where a gradient-enhanced damage formulation has been applied. The same test is also investigated by Aldakheel et al. [3], where a modified Gurson-type plasticity is used, coupled with the type of phase-field formulation discussed in 3.1.4. However, using that type of formulation, the crack starts to grow from the

Table 2 Material parameters used in the numerical simulations for the double-notched specimen

Symbol	Name	Value	Unit
K	Bulk modulus	194883.0	MPa
μ	Shear modulus	90000.0	MPa
σ_0	Initial yield stress	1073.47	MPa
σ_∞	Ultimate stress	1289.57	MPa
h	Linear hardening	67.22	MPa
ζ	Saturation parameter	1394.84	–
ψ_{cr}^p	Critical plastic fracture threshold	60.0	MPa·mm
g_c	Griffith constant	10.0	MPa·mm
l_f	Crack surface length scale	0.2	mm
κ	Interface mobility parameter	11700	MPa·s

**Fig. 3** **a** Evolution of accumulative plastic strain α and **b** phase-field parameter d for applied displacements of (1) 0.056 mm and (2) 0.152 mm in the tensile test of a double-notched specimen

upper notch first toward the upper surface, and then turns toward the lower part of the lower notch as depicted in Fig. 4 by black lines. This deviation in the crack pattern could be associated to the local irreversibility condition governed by Aldakheel et al. [3], which appears to drive the crack in a deviated direction. In contrast, the formulation provided in this paper does not require a local irreversibility constraint and thus, allows for a correction of the diffuse damage parameter fields yielding a correct crack path.

4.2 Tensile test of a dogbone-shaped specimen

The second benchmark problem investigated in this paper is a uniaxial tensile test of a dogbone-shaped specimen with an initial hole. The geometry of this specimen is depicted in Fig. 5. The 3D specimen with the thickness $t = 0.1$ mm, is subject to an external displacement $\bar{u} = 0.12$ mm, which is adaptively increased at the top surface in 476 load steps. The bottom of the specimen is fixed in all directions. Furthermore, there is

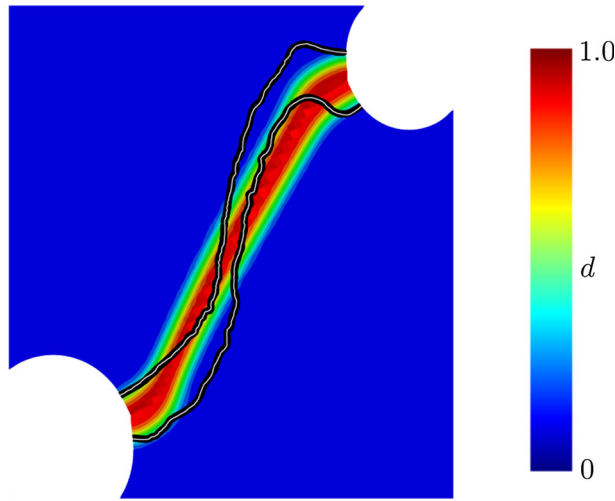


Fig. 4 Comparison of the crack path using the proposed formulation in this paper (colored path) versus the path (black lines) predicted using the formulation proposed by Aldakheel et al. [3]. (Color figure online)

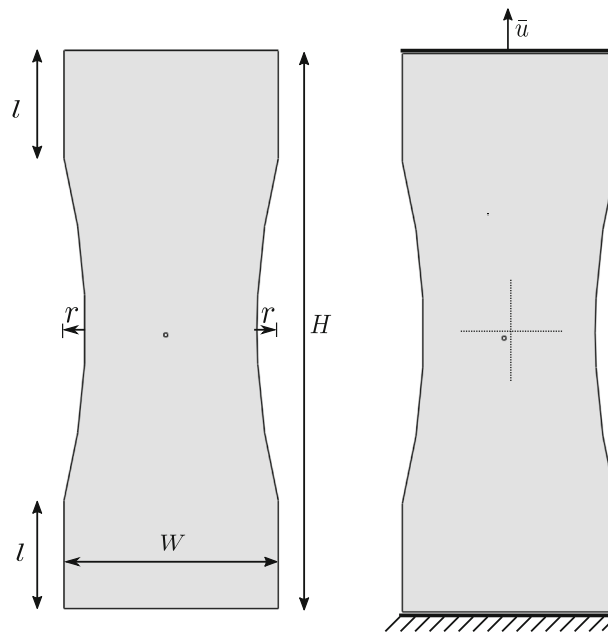


Fig. 5 Geometry of a dogbone-shaped specimen (left) with an unsymmetrically placed initial hole and boundary conditions (right)

a hole close to the center of the specimen with a rectangular cross-section of 0.1 by 0.1 mm. The geometrical dimensions of the specimen are given in Table 3. The maximum characteristic element length in this simulation is $h_e = 0.1$ mm and the considered material parameters are provided in Table 4. For the simulations, 72528 finite elements are used for the discretization of the specimen.

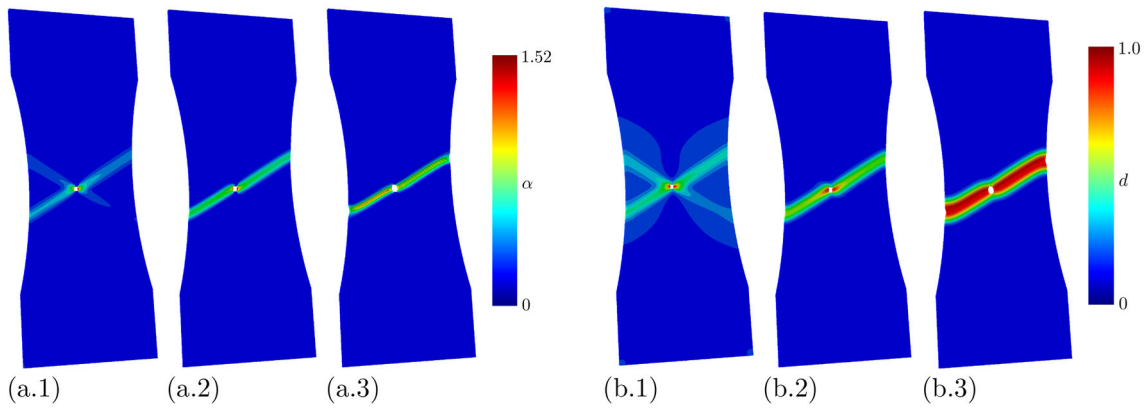
At the beginning of the process, the accumulative plastic strain α starts to evolve in the vicinity of the hole in the diagonal directions. It forms diagonal shear bands, as shown in Fig. 6a. The phase-field parameter evolves at a low rate in a very diffuse manner in the entire model depicted in Fig. 6d. By increasing the applied displacement, the accumulative plastic strains start to get localized in one of the diagonal directions, as shown in Fig. 6b, which is due to the fact that a slight asymmetry is included through the non-perfectly centered position of the initial hole. As a consequence, the phase-field parameter also starts getting localized within this diagonal band, as shown in Fig. 6e. Upon further stretching the specimen, the accumulative plastic strain is further localized within this band (Fig. 6c). The phase-field parameter reaches the value $d = 1$ in the vicinity of

Table 3 Geometrical dimensions of the dogbone-shaped specimen

Geometrical parameter	Value in mm
H	7.86
t	0.1
W	3.0
l	1.5
r	0.3

Table 4 Material parameters used in the numerical simulation of a dogbone-shaped specimen

Symbol	Name	Value	Unit
K	Bulk modulus	194883.0	MPa
μ	Shear modulus	90000.0	MPa
σ_0	Initial yield stress	1073.47	MPa
σ_∞	Ultimate stress	1289.57	MPa
h	Linear hardening	67.22	MPa
ζ	Saturation parameter	1394.84	–
ψ_{cr}^p	Critical plastic fracture threshold	85.0	MPa·mm
g_c	Griffith constant	8.0	MPa·mm
l_f	Crack surface length scale	0.1	mm
κ	Interface mobility parameter	10000	MPa·s

**Fig. 6** Evolution of **a** accumulative plastic strains α and **b** phase-field parameter d for applied external displacements of (1) 0.051 mm, (2) 0.064 mm, and (3) 0.085 mm in the tensile test of a dogbone-shaped specimen

the hole. It evolves within the diagonal shear band (Fig. 6f), as was expected from experimental and numerical observations, cf. [50] and [72]. Moreover, away from this region, the phase-field parameter reduces back to zero. Additionally, the simulation is repeated for varying numbers of elements and the reaction forces in the clamped edges are plotted over the applied displacements. Interestingly, the results as shown in Fig. 7 do not converge despite the relatively large number of finite elements, although regularization in terms of the phase-field approach is included. The convergence is studied for two further, different values of the mobility, i.e., $\kappa = 2000$ MPa·s and $\kappa = 50000$ MPa·s. As can be seen in the according results shown in Figs. 8 and 9, larger values of κ lead to a slower rate of crack propagation. Similarly, Kuhn and Müller [35] have studied the effect of the mobility parameter and observed that larger values of κ delays the start of crack propagation in brittle materials. As already observed in [72], the unregularized formation of localized shear bands leads to mesh-dependent results even if a mesh-independent crack propagation approach is considered. This turns out to be even independent on the choice of the mobility parameter and thus, on the viscosity of the damage evolution. The reason is that due to the specific boundary value problem, there may already be localized accumulations of plastic strains even before a crack evolves or propagates. Then, the regularization of crack propagation in terms of phase-field fracture does not help with the localized plastic strains. This motivates to extend the plasticity model by a micromorphic formulation, which is analyzed in the following section.

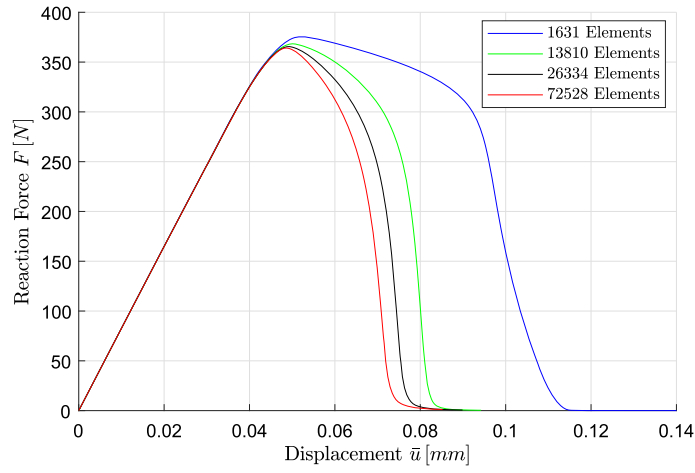


Fig. 7 Resultant reaction force at clamped boundary versus applied displacements for $\kappa = 10000$ MPa.s. A mesh-dependency is observed

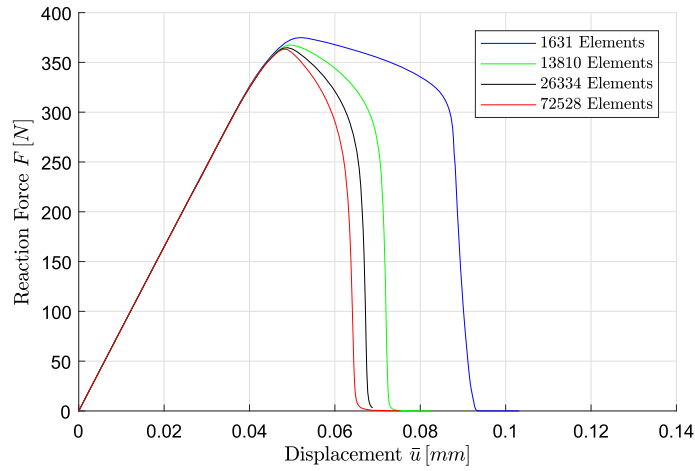


Fig. 8 Resultant reaction force at clamped boundary versus applied displacement for $\kappa = 2000$ MPa.s. A mesh-dependency is observed

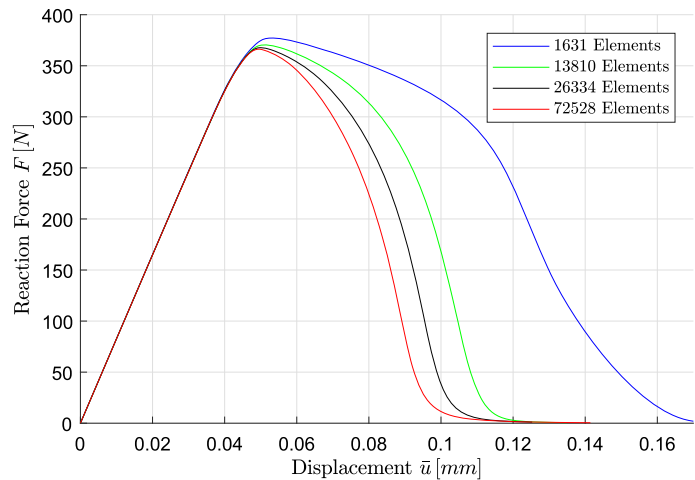
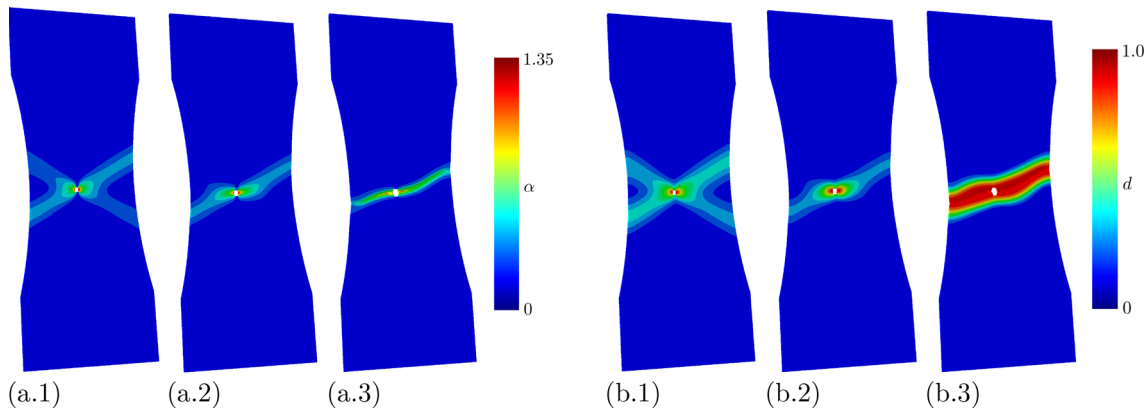


Fig. 9 Resultant reaction force at clamped boundary versus applied displacements for $\kappa = 50000$ MPa.s. A mesh-dependency is observed

Table 5 Material parameters used in the numerical simulations with the micromorphic extension

Symbol	Name	Value	Unit
K	Bulk modulus	194883.0	MPa
μ	Shear modulus	90000.0	MPa
σ_0	Initial yield stress	1073.47	MPa
σ_∞	Ultimate stress	1289.57	MPa
h	Linear hardening	67.22	MPa
ζ	Saturation parameter	1394.84	–
ψ_{cr}^p	Critical plastic fracture threshold	70	MPa·mm
g_c	Griffith constant	7.0	MPa·mm
l_f	Crack surface length scale	0.1	mm
χ	Micromorph constant	1600	MPa
l_p	Micromorph length scale	0.065	mm
κ	Interface mobility parameter	6000	MPa·s

**Fig. 10** Evolution of **a** accumulative plastic strains α and **b** phase-field parameter d for applied external displacements of (1) 0.06 mm, (2) 0.08 mm, and (3) 0.096 mm in the tensile test of a dogbone-shaped specimen using the micromorphic extension

4.3 Tensile test using micromorphic extension

To evaluate the formulation with the micromorphic extension, an 8-node user element with five nodal degrees of freedom has been implemented, where the global field $\tilde{\alpha}$ is the fifth nodal degree of freedom. The numerical experiment for a dogbone-shaped specimen is repeated here using the same geometry, where the material properties provided in Table 5 are chosen such that one can compare the FE-convergence curves with and without the micromorphic extension. As a result of the micromorphic extension, the localization of the shear bands is reduced. Furthermore, it is observed that the crack propagates again in an almost diagonal direction, however, with a lower slope, see Fig. 10. Again, the analysis is performed for different numbers of elements and the curve of the reaction forces at the clamped boundary versus the applied displacements is plotted in Fig. 11. When using the micromorphic extension, the localization of shear bands is appropriately regularized such that a mesh-independent crack propagation can be calculated using the proposed phase-field approach.

5 Conclusion

In this work, a new phase-field fracture framework based on the Allen–Cahn theory of diffusive interfaces has been introduced and successfully tested. The framework is based on the model initially proposed by Miehe et al. [47]. In the proposed formulation, a new definition of the phase-field parameter d is provided, where the bulk material is split into two parts which are separated by an interface. That is, the intact domain is characterized with $d = 0$, the fully cracked domain with $d = 1$ and the crack surface is specifically considered to be diffuse with $0 \leq d \leq 1$, respectively. Additionally, the crack surface energy is defined by a classical Modica–Mortola-type functional, which is known to be Γ -convergent. This type of definition is in agreement with the excess interface energy of the Allen–Cahn theory of diffuse interfaces. Furthermore, it is shown that the global irreversibility of the phase-field parameter is automatically fulfilled within this modified framework. In other words, healing

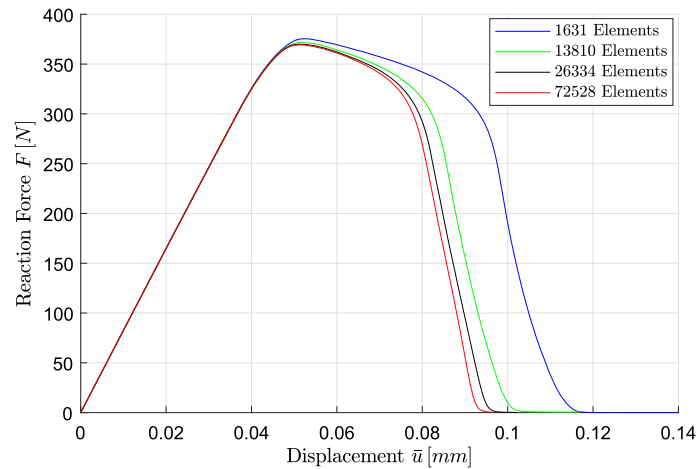


Fig. 11 Resultant reaction force at clamped boundary versus applied displacements. When using the micromorphic extension, clearly, mesh convergence can be obtained

of the crack is not allowed automatically and no local irreversibility constraint is needed. This formulation results in a phase-transition problem where only the intact phase can transform into the fully cracked phase. This modified formulation not only fulfills the balance of micromechanical forces but was also shown to be thermodynamically consistent in a nonlocal sense. Specifically for ductile problems, where localization of plastic strains may precede crack propagation and thus lead to mesh-dependent results, a micromorphic extension of the plasticity model has been included. Numerical analysis of the proposed formulation in several benchmark problems has shown that indeed reasonable, mesh-independent ductile crack propagation results can be achieved. It has been furthermore shown that crack path deviations, which may be caused by overly rigid local irreversibility constraints, can be avoided with the proposed approach.

Acknowledgements Hereby, the authors H. Montazer Hojjat and D. Balzani would like to appreciate financial funding by the Deutsche Forschungsgemeinschaft (DFG) in the framework of the Collaborative Research Center 837 (SFB 837), Project C6 "Interaction Modeling in Mechanized Tunneling". The first author would like to thank to the chief executive officer of the SFB 837, Jörg Sahlmen, for his kind support during the stay at Ruhr University Bochum. The author S. Kozinov would like to thank the DFG for funding under Grant KO 6356/1-1.

Declarations

Conflict of interest The authors declare that they have no conflicts of interest and did not involve human or animal participants in their study.

Appendix

A Continuum mechanical framework for ductile materials

Here, the continuum mechanical basis for the phase field model proposed in this paper as well as the considered elasto-plastic material model are described. Generally, a fictitiously undamaged strain energy density functional ψ_0 , defined per unit reference volume, can be written as a function of a deformation gradient $\mathbf{F} = \text{Grad}_X(\boldsymbol{\varphi}) = \nabla_X \boldsymbol{\varphi}$. The deformation mapping $\boldsymbol{\varphi}$ maps the point $\mathbf{X} \in \Omega$ in the reference (undeformed) configuration to the point $\mathbf{x} \in \boldsymbol{\varphi}(\Omega)$ in the current (deformed) configuration. In addition, the plastic deformation is an inelastic stress-free process. Therefore, an intermediate stress-free configuration is considered, which results in a multiplicative decomposition of the deformation gradient into a plastic and elastic one, i.e.,

$$\mathbf{F} = \mathbf{F}^e \cdot \mathbf{F}^p, \quad (55)$$

cf. [40]. Based on this decomposition, it is clear that the plastic deformation gradient has no contribution to the stored elastic energy. Furthermore, in some materials such as metals, the plastic deformation is volume

preserving, i.e., $\det(\mathbf{F}^P) = 1$. Therefore, the plastic incompressibility condition has to be satisfied. The strain energy density can thus be decomposed additively into an elastic and plastic term

$$\psi_0(\mathbf{F}, \mathbf{F}^P, \alpha) = \psi_0^e(\mathbf{F}, \mathbf{F}^P) + \psi_0^p(\alpha). \quad (56)$$

Herein, α is a strain-like internal variable. To fulfill objectivity, the elastic part is rewritten as a function of the elastic right Cauchy-Green tensor $\mathbf{C}^e = \mathbf{F}^{eT} \cdot \mathbf{F}^e = \mathbf{F}^{P^{-T}} \cdot \mathbf{C} \cdot \mathbf{F}^{P^{-1}}$ with the right Cauchy-Green tensor $\mathbf{C} := \mathbf{F}^T \cdot \mathbf{F}$, such that $\psi_0^e = \psi_0^e(\mathbf{F}^{eT} \cdot \mathbf{F}^e) = \psi_0(\mathbf{C}^e)$. By means of the postulate of minimum total potential energy and assuming conservative external forces, the deformation mapping is computed by

$$\boldsymbol{\varphi} = \arg \left\{ \inf \left(\int_{\Omega} \psi_0(\mathbf{C}^e, \alpha) \, dV - \int_{\Omega} \rho_0 \mathbf{b} \cdot \boldsymbol{\varphi} \, dV - \int_{\partial_N \Omega} \mathbf{T} \cdot \boldsymbol{\varphi} \, dA \right) \right\}, \quad (57)$$

where ρ_0 , $\rho_0 \mathbf{b}$, \mathbf{T} are the material density in reference configuration, body forces and the traction vector, respectively. Considering the second law of thermodynamics for isothermal conditions

$$\mathcal{D} = \mathbf{P}_0 : \dot{\mathbf{F}} - \dot{\psi}_0 \geq 0, \quad (58)$$

with the first Piola–Kirchhoff stress tensor \mathbf{P}_0 . Inserting the time derivative of ψ_0 yields

$$\left(\mathbf{P}_0 - \frac{\partial \psi_0}{\partial \mathbf{F}} \right) : \dot{\mathbf{F}} - \frac{\partial \psi_0}{\partial \mathbf{F}^P} : \dot{\mathbf{F}}^P - \frac{\partial \psi_0}{\partial \alpha} \dot{\alpha} \geq 0. \quad (59)$$

Applying the Coleman–Noll procedure leads to the constitutive equation for the first Piola–Kirchhoff stress tensor

$$\mathbf{P}_0 = \frac{\partial \psi_0^e}{\partial \mathbf{F}} = \mathbf{P}_0^e \cdot \mathbf{F}^{P^{-T}} \quad (60)$$

wherein $\mathbf{P}_0^e := \partial_{\mathbf{F}^e} \psi_0^e$ and $\partial_{\mathbf{F}} \mathbf{F}^e = \mathbf{F}^{P^{-T}}$. Defining the Mandel stress tensor [44] in the intermediate configuration $\boldsymbol{\Sigma}^e = \mathbf{F}^{eT} \cdot \mathbf{P}^e$ and the plastic spatial velocity gradient $\mathbf{L}^P = \dot{\mathbf{F}}^P \cdot \mathbf{F}^{P^{-1}}$ yields the reduced dissipation inequality

$$\mathcal{D} = \boldsymbol{\Sigma}^e : \mathbf{L}^P - Q \dot{\alpha} \geq 0, \quad (61)$$

where Q is the thermodynamic force of the internal variable α , i.e.,

$$Q := \frac{\partial \psi_0}{\partial \alpha} = \frac{\partial \psi_0^p}{\partial \alpha}. \quad (62)$$

For the description of elasto-plasticity, an admissible domain is defined in terms of the yield function $\phi \leq 0$. If the yield function is less than zero, i.e., $\phi < 0$, no plastic deformation takes place [43]. Furthermore, $\phi = 0$ represents the yield surface, where plastic deformations evolve. In case of metal plasticity with isotropic hardening, this state function is considered to have the form

$$\phi(\boldsymbol{\Sigma}^e, Q) := \|\text{dev} \boldsymbol{\Sigma}^e\| - Q. \quad (63)$$

Application of the principle of maximum dissipation and considering an associative flow rule, the evolution equations are obtained as

$$\mathbf{L}^P = \dot{\lambda} \mathbf{N}, \quad \dot{\lambda} = \dot{\alpha}, \quad (64)$$

where $\mathbf{N} := \partial_{\boldsymbol{\Sigma}^e} \phi$ is a second-order tensor imposing a constraint on the direction of plastic deformation and λ is the plastic multiplier. Applying the principle of maximum dissipation yields the well-known Kuhn-Tucker conditions

$$\dot{\lambda} \geq 0, \quad \dot{\lambda} \dot{\phi} \geq 0, \quad (65)$$

which need to be fulfilled. In order to fulfill the plastic incompressibility condition observed in metals, exponential integration is often used, cf. de Souza Neto [14]. An alternative can be obtained by noting that the

plastic incompressibility condition is automatically fulfilled if N is traceless [27]. In our model this will be the case. As a specification of the model, we consider a Neo-Hookean type energy density function

$$\psi_0^e = \frac{\mu}{2} (\text{tr}(\mathbf{C}^e) - 3) + \lambda \frac{J^{e^2} - 1}{4} - \left(\frac{\lambda}{2} + \mu \right) \ln(J^e), \quad J^e = \det(\mathbf{F}^e) > 0. \quad (66)$$

The plastic energy density is assumed to have the form [68]

$$\psi_0^p = \frac{1}{2} h \alpha^2 + (\sigma_\infty - \sigma_y) \left[\alpha + \frac{\exp(-\zeta \alpha) - 1}{\zeta} \right] + \sigma_y \alpha, \quad (67)$$

considering a saturation parameter ζ , a linear hardening parameter h , the initial yield stress σ_y , and a further parameter σ_∞ , which is associated with the modeling of the transition between an initially negative exponential hardening to a linear hardening. Note that the method proposed in this paper is not restricted to this choice of ψ_0^e and ψ_0^p .

B Details of phase-field modeling for brittle fracture

For the case of a hyperelastic material, the stored energy can be obtained by multiplying the degradation function with the Helmholtz free energy density of the intact material ψ_0 . This leads to the stored energy of the body given by

$$E(\mathbf{F}, d) = \int_{\Omega} g(d) \psi_0(\mathbf{F}) \, dV, \quad (68)$$

Moreover, using the chain rule and the time derivative of (68), the rate of degraded stored energy reads

$$\mathcal{E}(\mathbf{F}, d, \dot{\mathbf{F}}, \dot{d}) = \int_{\Omega} (\mathbf{P} : \dot{\mathbf{F}} - f^f \dot{d}) \, dV, \quad (69)$$

where the first Piola–Kirchhoff stress tensor is given by $\mathbf{P} = g(d) \mathbf{P}_0$. The fracture driving force f^f being the work conjugate to the phase-field parameter [22,47] reads

$$f^f := -\frac{\partial \psi}{\partial d} = -g'(d) \psi_0. \quad (70)$$

In addition, considering the long and short-range forces acting on the body, the external power is obtained as

$$\mathcal{P} = \int_{\Omega} \rho_0 \mathbf{b} \cdot \dot{\boldsymbol{\varphi}} \, dV + \int_{\partial_N \Omega} \mathbf{T} \cdot \dot{\boldsymbol{\varphi}} \, dA. \quad (71)$$

Furthermore, the regularized crack surface energy is defined using the critical fracture energy constant g_c . This energy is required to convert a fully intact matter into a fully cracked one. Considering constant g_c and the crack surface density functional, the crack energy is obtained

$$D(d) = \int_{\Omega} g_c \gamma(d, \nabla d) \, dV. \quad (72)$$

Therefore, using the time derivative and the chain rule, the dissipation functional \mathcal{D} for elastic materials reads

$$\mathcal{D}(\dot{d}) = \int_{\Omega} g_c \dot{\gamma} \, dV = \int_{\Omega} g_c \frac{\partial \gamma}{\partial d} \dot{d} \, dV, \quad (73)$$

where according to the second law of thermodynamics, only the non-negative values of the dissipation functional are admissible, i.e., $\mathcal{D}(\dot{d}) \geq 0$. Furthermore, Miehe et al. [47] enforced an irreversibility condition locally by defining a ramp-type energy function, that explodes for a negative evolution of the phase-field parameter. That means, the phase-field parameter is not allowed to reduce at any material point. Furthermore, the derivative of the crack surface density functional with respect to the phase-field parameter reads

$$\frac{\partial \gamma}{\partial d} = \frac{1}{l_s} \left(d - l_f^2 \Delta d \right), \quad (74)$$

where Δd is the material Laplacian of the phase-field parameter. At this stage, using the rate of stored energy functional (69), the external power (71) and the dissipation functional (73), the balance of mechanical power can be described as

$$\Pi(\dot{\phi}, \dot{d}) := \mathcal{E}(\dot{\phi}, \dot{d}) + \mathcal{D}(\dot{d}) - \mathcal{P}(\dot{\phi}). \tag{75}$$

Hence, the rates of deformation and damage parameter can be obtained from the variational principle

$$(\dot{\phi}, \dot{d}) = \arg\left\{ \inf_{\dot{\phi} \in \mathcal{W}_\phi} \inf_{\dot{d} \in \mathcal{W}_d} \Pi(\dot{\phi}, \dot{d}) \right\}, \tag{76}$$

where the following Dirichlet-type boundary condition is satisfied for the state variables

$$\dot{\phi} \in \mathcal{W}_\phi := \left\{ \dot{\phi} \mid \dot{\phi} = \mathbf{0} \text{ on } \partial_N \Omega_\phi \right\} \quad \text{and} \quad \dot{d} \in \mathcal{W}_d := \left\{ \dot{d} \mid \dot{d} = 0 \text{ on } \partial_N \Omega_d \right\}. \tag{77}$$

The variation of the balance of mechanical power leads to two equations: the balance of linear momentum

$$\text{Div } \mathbf{P} + \rho_0 \mathbf{b} = \mathbf{0}. \tag{78}$$

and the Kuhn–Tucker complementary conditions $\dot{d} \geq 0$, $f^f - g_c \delta_d \gamma \leq 0$, and $(f^f - g_c \delta_d \gamma) \dot{d} = 0$. That means the crack does not propagate as soon as $f^f - g_c \delta_d \gamma < 0$. On the other hand, as soon as the driving force reaches the critical value $f^f = g_c \delta_d \gamma$, the crack propagates. Remembering $f^f = -g'(d)\psi_0$, i.e., (70), the case distinction can be formulated as

$$\begin{cases} \dot{d} = 0 & \text{if } -g'(d)\psi_0 - g_c \delta_d \gamma < 0, \\ \dot{d} > 0 & \text{if } -g'(d)\psi_0 = g_c \delta_d \gamma. \end{cases} \tag{79}$$

Due to the local irreversibility, this type of formulation may lead to an unrealistic evolution of the phase-field parameter far away from the localization area in the case of ductile fracture. Moreover, May et al. [45] have shown numerically that discretized forms of such type of formulation are not necessarily Γ -convergent. This is also rooted in the local irreversibility condition, see [42]. This flaw was to some extent removed in Miehe et al. [50] by considering a fracture energy threshold. This threshold is imposed by a material constant w_c . That means, the phase-field parameter would evolve just in the material points, which possess energies beyond this threshold. Furthermore, the local irreversibility constraint is only enforced within this region which will vary throughout the crack formation in the general case. Taking this threshold into account, the thermodynamic force in (70) is modified to

$$f^f := -g'(d)(\psi_0 - w_c). \tag{80}$$

This formulation is sensitive to the definition of the material parameter w_c . In other words, the phase-field parameter would only evolve in the region, primarily determined by this material parameter. Not only this, but also the damage parameter is not allowed to get more localized within this region. Additionally, the discrete form of this formulation is not proven to be Γ -convergent.

References

1. ABAQUS/Standard. Dassault Systèmes Simulia Corp, Providence, RI (2022)
2. Aldakheel, F., Kienle, D., Keip, M.-A., Miehe, C.: Phase field modeling of ductile fracture in soil mechanics. *PAMM* **17**(1), 383–384 (2017). <https://doi.org/10.1002/pamm.201710161>
3. Aldakheel, F., Wriggers, P., Miehe, C.: A modified Gurson-type plasticity model at finite strains: formulation, numerical analysis and phase-field coupling. *Comput. Mech.* **62**(4), 815–833 (2018). <https://doi.org/10.1007/s00466-017-1530-0>
4. Allen, S.M., Cahn, J.W.: A microscopic theory for antiphase boundary motion and its application to antiphase domain coarsening. *Acta Metall.* **27**(6), 1085–1095 (1979). [https://doi.org/10.1016/0001-6160\(79\)90196-2](https://doi.org/10.1016/0001-6160(79)90196-2)
5. Ambati, M., Gerasimov, T., De Lorenzis, L.: Phase-field modeling of ductile fracture. *Comput. Mech.* **55**(5), 1017–1040 (2015). <https://doi.org/10.1007/s00466-015-1151-4>

6. Ambati, M., Kruse, R., De Lorenzis, L.: A phase-field model for ductile fracture at finite strains and its experimental verification. *Comput. Mech.* **57**(1), 149–167 (2015). <https://doi.org/10.1007/s00466-015-1225-3>
7. Balzani, D., Ortiz, M.: Relaxed incremental variational formulation for damage at large strains with application to fiber-reinforced materials and materials with truss-like microstructures. *Comput. Methods Appl. Mech. Eng.* **92**, 551–570 (2012)
8. Belytschko, T., Black, T.: Elastic crack growth in finite elements with minimal remeshing. *Int. J. Numer. Methods Eng.* **45**(5), 601–620 (1999)
9. Borden, M.J., Hughes, T.J., Landis, C.M., Anvari, A., Lee, I.J.: A phase-field formulation for fracture in ductile materials: finite deformation balance law derivation, plastic degradation, and stress triaxiality effects. *Comput. Methods Appl. Mech. Eng.* **312**, 130–166 (2016). <https://doi.org/10.1016/J.CMA.2016.09.005>
10. Bourdin, B.: Numerical implementation of the variational formulation for quasi-static brittle fracture. *Interfaces Free Bound.* **9**, 411–430 (2007). <https://doi.org/10.4171/IFB/171>
11. Braides, A.: *Gamma-Convergence for Beginners*. Oxford University Press, London (2002). <https://doi.org/10.1093/acprof:oso/9780198507840.001.0001>
12. Cahn, J.W., Hilliard, J.E.: Free energy of a nonuniform system. I. Interfacial free energy. *J. Chem. Phys.* **28**(2), 258–267 (1958). <https://doi.org/10.1063/1.1744102>
13. Cornetti, P., Pugno, N., Carpinteri, A., Taylor, D.: Finite fracture mechanics: a coupled stress and energy failure criterion. *Eng. Fract. Mech.* **73**(14), 2021–2033 (2006). <https://doi.org/10.1016/j.engfracmech.2006.03.010>
14. de Souza Neto, E.: The exact derivative of the exponential of an unsymmetric tensor. *Comput. Methods Appl. Mech. Eng.* **190**(18–19), 2377–2383 (2001). [https://doi.org/10.1016/S0045-7825\(00\)00241-3](https://doi.org/10.1016/S0045-7825(00)00241-3)
15. Dimitrijevic, B., Hackl, K.: A method for gradient enhancement of continuum damage models. *Tech. Mech.* **28**(1), 43–52 (2008)
16. Dimitrijevic, B.J., Hackl, K.: A regularization framework for damage-plasticity models via gradient enhancement of the free energy. *Int. J. Numer. Methods Biomed. Eng.* **27**(8), 1199–1210 (2011). <https://doi.org/10.1002/cnm.1350>
17. Duda, F.P., Ciaronetti, A., Sánchez, P.J., Huespe, A.E.: A phase-field/gradient damage model for brittle fracture in elastic-plastic solids. *Int. J. Plast.* **65**, 269–296 (2015). <https://doi.org/10.1016/j.ijplas.2014.09.005>
18. Eringen, A.C., Suhubi, E.: Nonlinear theory of simple micro-elastic solids–i. *Int. J. Eng. Sci.* **2**(2), 189–203 (1964). [https://doi.org/10.1016/0020-7225\(64\)90004-7](https://doi.org/10.1016/0020-7225(64)90004-7)
19. Forest, S.: Micromorphic approach for gradient elasticity, viscoplasticity, and damage. *J. Eng. Mech.* **135**(3), 117–131 (2009). [https://doi.org/10.1061/\(ASCE\)0733-9399\(2009\)135:3\(117\)](https://doi.org/10.1061/(ASCE)0733-9399(2009)135:3(117))
20. Francfort, G.A., Marigo, J.J.: Revisiting brittle fracture as an energy minimization problem. *J. Mech. Phys. Solids* **46**(8), 1319–1342 (1998). [https://doi.org/10.1016/S0022-5096\(98\)00034-9](https://doi.org/10.1016/S0022-5096(98)00034-9)
21. Griffith, A.A.: The phenomena of rupture and flow in solids. *Philos. Trans. R. Soc. Lond. Ser. A* **221**, 163–198 (1921)
22. Gültekin, O., Dal, H., Holzapfel, G.A.: A phase-field approach to model fracture of arterial walls: theory and finite element analysis. *Comput. Methods Appl. Mech. Eng.* **312**, 542–566 (2016). <https://doi.org/10.1016/j.cma.2016.04.007>
23. Gültekin, O., Dal, H., Holzapfel, G.A.: Numerical aspects of anisotropic failure in soft biological tissues favor energy-based criteria: a rate-dependent anisotropic crack phase-field model. *Comput. Methods Appl. Mech. Eng.* **331**, 23–52 (2018). <https://doi.org/10.1016/j.cma.2017.11.008>
24. Gurtin, M.E.: Generalized Ginzburg–Landau and Cahn–Hilliard equations based on a microforce balance. *Phys. D* **92**(3–4), 178–192 (1996). [https://doi.org/10.1016/0167-2789\(95\)00173-5](https://doi.org/10.1016/0167-2789(95)00173-5)
25. Hakim, V., Karma, A.: Laws of crack motion and phase-field models of fracture. *J. Mech. Phys. Solids* **57**(2), 342–368 (2009). <https://doi.org/10.1016/j.jmps.2008.10.012>
26. Hashin, Z.: Finite thermoelastic fracture criterion with application to laminate cracking analysis. *J. Mech. Phys. Solids* **44**(7), 1129–1145 (1996). [https://doi.org/10.1016/0022-5096\(95\)00080-1](https://doi.org/10.1016/0022-5096(95)00080-1)
27. Hurtado, D., Stainier, L., Ortiz, M.: The special-linear update: an application of differential manifold theory to the update of isochoric plasticity flow rules. *Int. J. Numer. Methods Eng.* **97**(4), 298–312 (2019). <https://doi.org/10.1002/nme.4600>
28. Inglis, C.E.: Stresses in a plate due to the presence of cracks and sharp corners. *Trans. Inst. Naval Archit.* **55**, 219–241 (1913)
29. Irwin, G.R.: Analysis of stresses and strains near the end of a crack traversing a plate. *Appl. Mech. Trans. ASME* **E24**, 351–369 (1957)
30. Junker, P., Schwarz, S., Jantos, D., Hackl, K.: A fast and robust numerical treatment of a gradient-enhanced model for brittle damage. *Int. J. Multiscale Comput. Eng.* **17**(2) (2019)
31. Junker, P., Riesselmann, J., Balzani, D.: Efficient and robust numerical treatment of a gradient-enhanced damage model at large deformations. *Int. J. Numer. Methods Eng.* **123**, 774–793 (2022). <https://doi.org/10.1002/nme.6876>
32. Karma, A., Kessler, D.A., Levine, H.: Phase-field model of mode III dynamic fracture. *Phys. Rev. Lett.* **87**(4), 045501 (2001). <https://doi.org/10.1103/PhysRevLett.87.045501>
33. Kirsch. Die theorie der elastizität und die bedürfnisse der festigkeitslehre. *Zeitschrift des Vereins deutscher Ingenieure*, pp. 797–807 (1898)
34. Köhler, M., Balzani, D.: Evolving microstructures in relaxed continuum damage mechanics for the modeling of strain softening. *J. Mech. Phys. Solids* **173**, 105199 (2023)
35. Kuhn, C., Müller, R.: A continuum phase field model for fracture. *Eng. Fract. Mech.* **77**(18), 3625–3634 (2010). <https://doi.org/10.1016/j.engfracmech.2010.08.009>
36. Kuhn, C., Schlüter, A., Müller, R.: On degradation functions in phase field fracture models. *Comput. Mater. Sci.* **108**, 374–384 (2015). <https://doi.org/10.1016/j.commatsci.2015.05.034>
37. Kuhn, C., Noll, T., Müller, R.: On phase field modeling of ductile fracture. *GAMM-Mitt.* **39**(1), 35–54 (2016). <https://doi.org/10.1002/gamm.201610003>
38. Langenfeld, K., Mosler, J.: A micromorphic approach for gradient-enhanced anisotropic ductile damage. *Comput. Methods Appl. Mech. Eng.* **360**, 112717 (2020). <https://doi.org/10.1016/j.cma.2019.112717>
39. Langenfeld, K., Kurzeja, P., Mosler, J.: How regularization concepts interfere with (quasi-)brittle damage: a comparison based on a unified variational framework. *Continuum Mech. Thermodyn.* **34**(6), 1517–1544 (2022). <https://doi.org/10.1007/s00161-022-01143-2>

40. Lee, E.: Elasto-plastic deformation at finite strains. *J. Appl. Mech.* **36**, 1–6 (1969)
41. Leguillon, D.: Strength or toughness? A criterion for crack onset at a notch. *Eur. J. Mech. A. Solids* **21**(1), 61–72 (2002). [https://doi.org/10.1016/S0997-7538\(01\)01184-6](https://doi.org/10.1016/S0997-7538(01)01184-6)
42. Linse, T., Hennig, P., Kästner, M., de Borst, R.: A convergence study of phase-field models for brittle fracture. *Eng. Fract. Mech.* **184**, 307–318 (2017). <https://doi.org/10.1016/j.engfracmech.2017.09.013>
43. Lubliner, J.: On the thermodynamic foundations of non-linear solid mechanics. *Int. J. Non-Linear Mech.* **7**(3), 237–254 (1972). [https://doi.org/10.1016/0020-7462\(72\)90048-0](https://doi.org/10.1016/0020-7462(72)90048-0)
44. J. Mandel. Plasticité classique et viscoplasticité. In: CISM Courses and Lectures No. 97. Springer (1972)
45. May, S., Vignollet, J., De Borst, R.: A numerical assessment of phase-field models for brittle and cohesive fracture: γ -convergence and stress oscillations. *Eur. J. Mech. A. Solids* **52**, 72–84 (2015)
46. Miehe, C., Schänzel, L.-M.: Phase field modeling of fracture in rubbery polymers. Part I: finite elasticity coupled with brittle failure. *J. Mech. Phys. Solids* **65**, 93–113 (2014). <https://doi.org/10.1016/j.jmps.2013.06.007>
47. Miehe, C., Welschinger, F., Hofacker, M.: Thermodynamically consistent phase-field models of fracture: variational principles and multi-field FE implementations. *Int. J. Numer. Methods Eng.* **83**(10), 1273–1311 (2010). <https://doi.org/10.1002/nme.2861>
48. Miehe, C., Schänzel, L.-M., Ulmer, H.: Phase field modeling of fracture in multi-physics problems part i balance of crack surface and failure criteria for brittle crack propagation in thermo-elastic solids. *Comput. Methods Appl. Mech. Eng.* **294**, 449–485 (2015). <https://doi.org/10.1016/j.cma.2014.11.016>
49. Miehe, C., Aldakheel, F., Raina, A.: Phase field modeling of ductile fracture at finite strains: a variational gradient-extended plasticity-damage theory. *Int. J. Plast.* **84**, 1–32 (2016). <https://doi.org/10.1016/j.ijplas.2016.04.011>
50. Miehe, C., Teichtmeister, S., Aldakheel, F.: Phase-field modelling of ductile fracture: a variational gradient-extended plasticity-damage theory and its micromorphic regularization. *Philos. Trans. R. Soc. A Math. Phys. Eng. Sci.* **374**(2066), 20150170 (2016). <https://doi.org/10.1098/rsta.2015.0170>
51. Mindlin, R.D.: Micro-structure in linear elasticity. *Arch. Ration. Mech. Anal.* **16**(1), 51–78 (1964). <https://doi.org/10.1007/BF00248490>
52. Modica, L., Mortola, S.: Un esempio di γ -convergenza. *Bollettino dell'Unione Matematica Italiana* **14–B**, 285–299 (1977)
53. Mosler, M., Shchyglo, O., Montazer Hojjat, H.: A novel homogenization method for phase field approaches based on partial rank-one relaxation. *J. Mech. Phys. Solids* **68**, 251–266 (2014). <https://doi.org/10.1016/j.jmps.2014.04.002>
54. Msekh, M.A., Sargado, J.M., Jamshidian, M., Areias, P.M., Rabczuk, T.: Abaqus implementation of phase-field model for brittle fracture. *Comput. Mater. Sci.* **96**, 472–484 (2014). <https://doi.org/10.1016/j.commatsci.2014.05.071>
55. Mughrabi, H.: Assessment of fatigue damage on the basis of nonlinear compliance effects. In: *Handbook of Materials Behavior Models*, pp. 622–632. Academic Press (2001)
56. Orowan, E.: Fracture and strength of solids. *Rep. Prog. Phys.* **12**(1), 185–232 (1949). <https://doi.org/10.1088/0034-4885/12/1/309>
57. Pandolfi, A., Ortiz, M.: An Eigenerosion approach to brittle fracture. *Int. J. Numer. Methods Eng.* **92**(8), 694–714 (2012). <https://doi.org/10.1002/nme.4352>
58. Polindara, C., Waffenschmidt, T., Menzel, A.: Simulation of balloon angioplasty in residually stressed blood vessels—application of a gradient-enhanced fibre damage model. *J. Biomech.* **49**(12), 2341–2348 (2016). <https://doi.org/10.1016/j.jbiomech.2016.01.037>
59. Proserpio, D., Ambati, M., De Lorenzis, L., Kiendl, J.: A framework for efficient isogeometric computations of phase-field brittle fracture in multipatch shell structures. *Comput. Methods Appl. Mech. Eng.* **372**, 113363 (2020). <https://doi.org/10.1016/j.cma.2020.113363>
60. Raina, A., Miehe, C.: A phase-field model for fracture in biological tissues. *Biomech. Model. Mechanobiol.* **15**(3), 479–496 (2015). <https://doi.org/10.1007/s10237-015-0702-0>
61. Riesselmann, J., Balzani, D.: A simple and efficient Lagrange multiplier based mixed finite element for gradient damage. *Comput. Struct.* **281**, 107030 (2023). <https://doi.org/10.1016/j.compstruc.2023.107030>
62. Schmidt, T., Balzani, D.: Relaxed incremental variational approach for the modeling of damage-induced stress hysteresis in arterial walls. *J. Mech. Behav. Biomed. Mater.* **58**, 149–162 (2016). <https://doi.org/10.1016/j.jmbbm.2015.08.005>
63. Seupel, A., Hütter, G., Kuna, M.: An efficient FE-implementation of implicit gradient-enhanced damage models to simulate ductile failure. *Eng. Fract. Mech.* **199**, 41–60 (2018). <https://doi.org/10.1016/j.engfracmech.2018.01.022>
64. Simo, J.C.S., Oliver, J., Armero, F.: An analysis of strong discontinuities induced by strain-softening in rate-independent inelastic solids. *Comput. Mech.* **12**(5), 277–296 (1993). <https://doi.org/10.1007/BF00372173>
65. Spetz, A., Denzer, R., Tudisco, E., Dahlblom, O.: Phase-field fracture modelling of crack nucleation and propagation in porous rock. *Int. J. Fract.* **224**, 31–46 (2020). <https://doi.org/10.1007/s10704-020-00444-4>
66. Steinbach, I.: Phase-field model for microstructure evolution at the mesoscopic scale. *Annu. Rev. Mater. Res.* **43**(1), 89–107 (2013). <https://doi.org/10.1146/annurev-matsci-071312-121703>
67. Torabi, A.R., Berto, F., Sapora, A.: Finite fracture mechanics assessment in moderate and large scale yielding regimes. *Metals* **9**(5), 602 (2019). <https://doi.org/10.3390/met9050602>
68. Voce, E.: A practical strain hardening function. *Metallurgia* **51**, 219–226 (1955)
69. Waffenschmidt, T., Polindara, C., Menzel, A., Blanco, S.: A gradient-enhanced large-deformation continuum damage model for fibre-reinforced materials. *Comput. Methods Appl. Mech. Eng.* **268**, 801–842 (2014). <https://doi.org/10.1016/j.cma.2013.10.013>
70. Weißgraeber, P., Leguillon, D., Becker, B.: A review of finite fracture mechanics: crack initiation at singular and non-singular stress raisers. *Arch. Appl. Mech.* **86**(1–2), 375–401 (2015). <https://doi.org/10.1007/s00419-015-1091-7>
71. Wingender, D., Balzani, D.: Simulation of crack propagation through voxel-based, heterogeneous structures based on Eigen-erosion and finite cells. *Comput. Mech.* **70**, 385–406 (2022). <https://doi.org/10.1007/s00466-022-02172-z>

-
72. Wingender, D., Balzani, D.: Simulation of crack propagation based on Eigenerosion in brittle and ductile materials subject to finite strains. *Arch. Appl. Mech.* (2022). <https://doi.org/10.1007/s00419-021-02101-1>

Publisher's Note Springer Nature remains neutral with regard to jurisdictional claims in published maps and institutional affiliations.

Springer Nature or its licensor (e.g. a society or other partner) holds exclusive rights to this article under a publishing agreement with the author(s) or other rightsholder(s); author self-archiving of the accepted manuscript version of this article is solely governed by the terms of such publishing agreement and applicable law.